國立交通大學

顯示科技研究所

碩士論文

交流型電漿顯示器之
氧化鎂保護層與面板特性之關係與研究

Relationship between MgO Thin Film Properties and Panel Performance in AC-PDP

研 究 生：李偉誠

指導教授：金星吾 教授

中華民國九十五年六月

交流型電漿顯示器之
氧化鎂保護層與面板特性之關係與研究

Relationship between MgO Thin Film Properties and Panel Performance in AC-PDP

研 究 生: 李偉誠　　Student: Wei-Cheng Lee

指導教授: 金星吾　　Advisor: Dr. Sung-O Kim

國立交通大學

顯示科技研究所

碩士論文

A Thesis

Submitted to Department of Photonics and Display Institute
College of Electrical Engineering and Computer Science
National Chiao-Tung University
in Partial Fulfillment of the Requirements
for the Degree of Master
in
Display

June 2006

Hsinchu, Taiwan, Republic of China.

中華民國九十五年六月

交流型電漿顯示器之
氧化鎂保護層與面板特性之關係與研究

研究生：李偉誠　　指導教授：金星吾 博士

國立交通大學顯示科技研究所

摘要

隨著電腦科技與網路普及所帶來對人類生活品質的衝擊，各樣具有輕薄短小、低耗功率等顯示器的需求越來越高，近年來更邁入大尺寸家用型電視市場。交流型電漿顯示器更成為家用型大型電視的最佳候選人。不需要背光模組的自發光特性、三十二至一百吋的大尺寸顯示畫面、輕薄懸掛式，以及高畫質電視等特性，都使得交流型電漿顯示器在這場家用大型電視的大戰中顯得格外的引人注目。然而，交流型電漿顯示器仍然有關鍵性的問題有待解決。烙痕現象以及顯示壽命以及消耗功率是現階段即待改善的關鍵議題。有鑒於傳統的交流型電漿顯示器對於氧化鎂保護層的特性以及面板特性之關係並無專門研究，在此我們將針對氧化鎂保護層對於烙痕現象以及面板表現的關係提出討論。

此研究的重點在於針對調整改氧化鎂在蒸鍍時的條件，並加以修正已達到產生出最佳化地保護層膜。以此提高其保護藉電層的功能與時效，以及進一步藉由其良好的特性提升電漿放電的效率，以達到改善交流型電漿顯示器在亮度、反應時間、消耗功率以及烙痕方面的缺點。

Relationship between MgO Thin Film Properties and Panel Performance in AC-PDP

Student: Wei-Cheng Lee **Advisor: Dr. Sung-O Kim**

Department of Photonics and Display Institute,
National Chiao Tung University

Abstract

The impact of MgO thin film properties on the performance of AC-Plasma Display Panels (AC-PDPs) is described. In this study, MgO thin films in AC-PDPs are deposited by e-beam evaporation in which the oxygen flow rate and electron beam current are varied. Properties of PDP, including luminance, response time, dynamic margin, and color temperature, image sticking are characterized as a function of time in accelerated aging tests. Besides, both surface analysis and theory demonstrate that a PDP incorporating MgO films grown at reduced O_2 flow rates provide improved panel properties due to a higher density of the MgO film, higher crystallinity and a uniform but relatively surface roughness. In this study, it reveals that MgO deposited with 10 sccm oxygen flow rate exhibits the highest thin film density compared to others. This high density MgO thin film with a uniform but relatively rough surface results in optimal luminance and good performance.

致謝

首先，我要感謝上帝賜給我這個機會能在交通大學的研究所當中學習，除了知識上的長進，更在人生歷練中往前一大步，感謝神的恩典與帶領。我還要感謝金星吾指導教授在學業、研究以及英文方面的指導，並且讓我在研究生活當中有更深的國際觀也在團隊當中學習到團隊精神與合作的重要。

除此之外，我要感謝四位與我一起打拼奮鬥的好伙伴們－吳正宇、周鴻杰、卓龍材以及任珂銳。第一屆的同袍情誼，讓我深深體會到知心好友的重要。謝謝你們在日常生活中的照顧與包容，更感謝你們在實驗上的幫助與鼓勵，兩年的共同生活讓我從你們身上有許多深刻的學習；我還要感謝實驗室助理張雅惠小姐的細心幫忙與協助；中華映管的陳孝生處長、李建邦經理、黃志明以及許建興工程師等在專業上面的協助。

最後但也是最重要的，我要感謝我親愛的父母以及弟弟，謝謝你們愛的包容與無私心的支持；我更要感謝我的女朋友王俐文，謝謝你陪我走過這段時光，感謝妳在低潮時的陪伴與鼓勵，感謝妳百分百的支持與愛，讓我能咬緊牙關完成研究所的課程與實驗；我要再一次感謝神賜給我這一切，讓這份喜悅與每位關心我的人分享。

Table of Contents

Figure Caption

List of Tables

Chapter 1

Introduction

As quality of life of human beings has been greatly valued in recent days, electronic products capable of light weight, thin volume and low power consumption are then spring up and highly demanded. Among those designs, Flat Panel Display (FPD) is unquestionably one of the most attractive products. In this chapter, the trend of development of FPDs and characteristics of Plasma Display Panel (PDPs) are briefly introduced and the objectives of the thesis will be resolved.

1.1 Flat Panel Display

Industry of FPD is now growing up rapidly due to the demand of consumer electronic product market. For different applications, such as TV, monitor, laptop computer, cell-phone, PDA, and digital camera, varied approaches have been adopted to achieve these goals. Generally, several well known technologies including Plasma Display Panel (PDP), Liquid Crystal Display (LCD), CRT (Cathode Ray Tube), Organic Light Emissive Device (OLED) are now the main stream among those approaches in the markets. Until recently, the market for direct-view, flat panel televisions was segmented fairly clearly, with LCD sets available only in screen sizes smaller than 50 inches, and PDP products available in larger screen sizes ranging from 37 to 103 inches. In the past decade, LCD has become the dominant answer for desktop and laptop computer monitors. The consumer market for these two flat panel technologies is beginning to converge, due to mass production of LCDs in larger screen sizes.

Nevertheless, it is believed that PDP is the promising candidate for the large sized TV and home theatre applications. Excellent image quality and necessary big size (more than 100 inches) give PDP the ability to fulfill the dream of building up home theatre in each family. Unlike LCD using Cold Cathode Fluorescent Lamp (CCFL) as a backlight source, PDP is a self-emissive display, which can provide wide viewing angle, makes it have a CRT like high image quality [1]. Without those complicated fabricating processes which have been used in LCDs, it only requires several simple technologies to fulfill the fabrication of a PDP module. Accordingly, the fundamental structure and basic working mechanism of PDPs will be introduced in the next paragraph.

1.2 Plasma Display Panel

Plasma displays are enjoying an unprecedented degree of success as large-screen televisions (TVs). World sales of plasma display modules reached $6 billion in 2005. Sales are projected to be $8.9 billion by 2007. Plasma TV products are now available in a range of screen diagonals from 32-inch to 80-inch. In the start of 2005, there shows the appearance of a high quality 102-inch diagonal 1920 x 1080 pixel high definition plasma TV prototype. The U.S. based Consumer Electronics Association's October 2004 holiday forecast survey found that plasma TV was the most desired gift for the holiday season [2].

While PDP and LCD offer some shared benefits (flat, thin form factor and undistorted, fixed-pixel image rendering), significant quality differences still remain. Plasma displays continue to best fill the needs of home theatre enthusiasts seeking premium-quality large-screen display devices, due to several inherent benefits of the technology.

The large area FPD is demanded for a HDTV and a digital TV which displays a real and life-size image in addition to the traditional TV image because of the development of the both computer and network technologies.

Fig. 1.1 "Now it is just starting to blossom," said Larry Weber of the consumer market for plasma display panel. The figure shows a sharp and bright image quality with a colorful flowers picture.

As shown in Fig. 1.1, PDP's image quality looks sharp and bright from virtually anywhere in the room. On the other hand, because plasma TV screens use the phosphor coating (like direct-view and projection CRT TVs), the potential for image burn-in exists, so it's important to follow the manufacturer's recommendations on day-to-day use. It is known that plasma TVs based on innovative AliS technology (Alternate Lighting of Surfaces) are proving that even a non-progressive picture can look outstanding [3].

1.2.1 Fundamental Structure

Fig. 1.2 shows the fundamental PDP structure which has been widely used for the TV markets in nowadays. As shown in the figure, a plasma display panel consists of two transparent glass panels (front and rear panel) with a thin layer of pixels sandwiched in between.

Since a plasma display panel is illuminated at the sub-pixel level, images are extremely accurate, and the panel's light output is both high and consistent across the entire screen area. Each individual plasma cell is switched on and off by its own electrode. An HDTV-capable PDP can have up to 3 million of these cells.

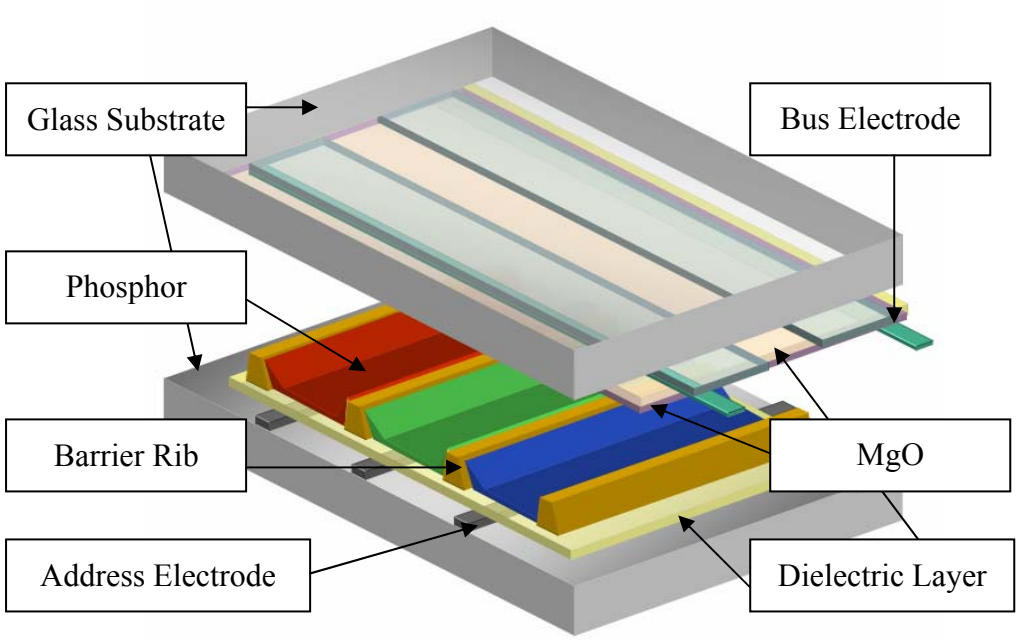

Fig. 1.2 Fundamental PDP structure widely used in the TV market application.

Fig. 1.3 illustrates the schematics of a PDP cell. Typical PDP has a strip of electrodes for each horizontal row of plasma cells. Pixels are separated by barrier ribs

and each of them is composed of three gas-filled cells or sub-pixels (Each cell, or pixel, actually consists of one red, one blue and one green sub-pixel).

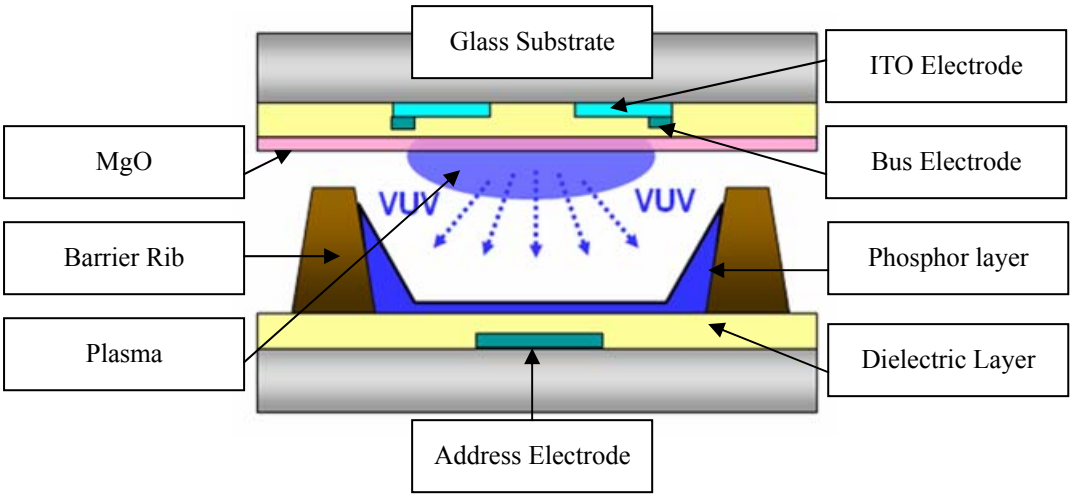

Fig. 1.3 Conventional PDP cell structure.

In the mass production line, conventional barrier ribs are fabricated by sandblasting method and the formation of barrier ribs is the key factor to make high resolution plasma TV. Three primary color phosphor materials for red, blue, and green colors are deposited in the neighboring channels made by the barrier ribs to cover both of the side wall of the ribs and the dielectric layer. Generally, phosphor materials are (Y.Ga)BO_3:Eu for red; $BaMgAl1_4O_{23}$:Eu for blue; and Zn_2SiO_4:Mn for green and deposited on the barrier ribs by screen printing method.

The substrates are assembled onto each other with about a 120 μm gap and the Ne + Xe gas mixture is introduced between each gap. A grid of electrodes deposited on dielectric layer applies an electric current to the individual cells, causing the gas in the selected cells to ionize plasma. In order to prevent the damage caused by ion bombardment, Magnesium Oxide (MgO) plays an important role as a protective layer

is deposited on the dielectric layer.

In a word, electricity sent through an array of electrodes that are in close proximity to the cells, excites the gas. This ionized gas (plasma) emits high-frequency VUV rays (147 and 173 nm) resulting in a discharge of ultraviolet light. The light then strikes a phosphor coating on the inside of the glass, which causes the emission of red, blue or green visible light. The three colors in each pixel combine according to the amount of electric pulses fed to each sub-pixel, (which varies according to the signals sent to the electrodes by the plasma display's internal electronics), to emit visible light and glow the desired image or color to observer's eyes.

1.3 Motivation and Objectives

As illustrated in Fig. 1.4, in order to protect the dielectric layer from the ion bombardment, Magnesium Oxide (MgO) as a protective layer becomes the critical material due to its exposure under the plasma in the cell. Electron-beam evaporated MgO films are usually used as the protecting layer for its high surface resistivity, high secondary electron emission coefficient (γ), good transparency, and strong sputtering resistance…etc. [4-6] The secondary electron emission coefficient of the MgO film is defined as the total number of ejected electrons per incident ion and is one of the important parameters that affect the firing and sustain voltages of an ac PDP [7]. As a result, it is believed that the performance of PDP is strongly influenced by the surface characteristics of MgO thin films because the film is exposed to the plasma.

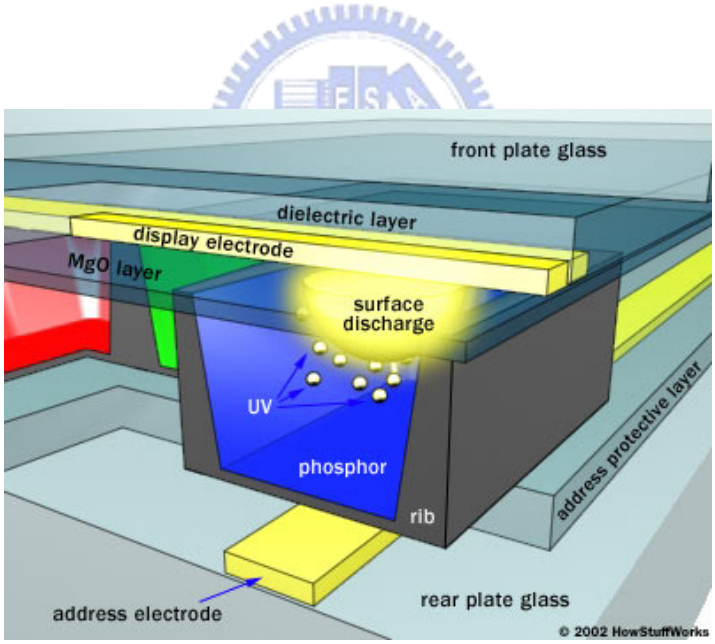

Fig. 1.4 The ionized gas discharge (plasma) generates vacuum ultraviolet (VUV) to stimulate the phosphor layer and emit visible light through the front panel. As shown in the figure, ion bombardment would reach to the dielectric layer which is protected by MgO [4].

In this work, MgO thin films are deposited by e-beam evaporation in which the

deposition parameters are designed particularly to investigate the relationship between MgO thin film properties and PDP panel performance. During the fabrication process, evaporation parameters including oxygen flow rate, electron beam current, chamber temperature, chamber pressure and tact time are selected to realize the experiment. Furthermore, properties of the PDP such as luminance, response time, dynamic and static margin, color temperature, CIE coordinates and image sticking phenomenon, are characterized as a function of time by demonstrating 46 inches WVGA type AC-PDP in accelerated aging tests. Both MgO thin film surface analysis and theory are also characterized in the following chapters.

1.4 Organization

Based on the concepts mentioned above, the objective of this thesis is to realize how the MgO thin film properties affect the PDP performance. Moreover, the PDP working mechanism and fabrication process will also be introduced. The experimental setup will be carried out firstly for the optimization and analyses; then, the investigation and comparison will be implemented to characterize the MgO thin film properties. This thesis is organized to review the basic theories and previous literatures in Chapter 2. Fabrication process and measurement instrument are described in Chapter 3. The experiments with results and discussions will be placed in Chapter 4 and following is the conclusion in Chapter 5.

Chapter 2

Principle of Plasma Display Panel

In chapter 2, the basic knowledge of PDP will be introduced, including PDP history, theory of gas discharge (plasma), fabrication process, and the key materials adopted in plasma display panels. Furthermore, the most critical material MgO thin film as a protective layer will be particularly surveyed in the final section of this chapter.

2.1 PDP History

The plasma display panel was invented at the University of Illinois at Urbana-ChampaignT (UIUC) by Donald L. Bitzer and H. Gene Slottow (shown in Fig. 2.1) in 1964 for the need for a high quality display for computer-based education, PLATO (Programmed Logic for Automatic Teaching Op-erations) Computer System [8].

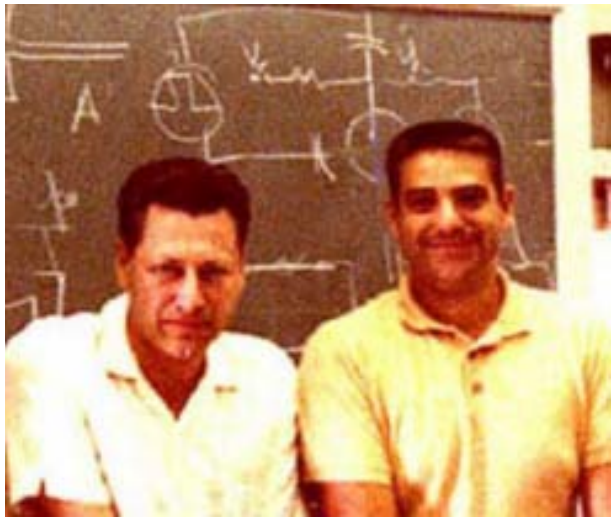

Fig. 2.1 The inventor of plasma display panel: Prof. H. Gene Slottow (left) and Prof. Donald L. Bitzer at the University of Illinois in 1967 [8].

Looking back, it was an innovating proposal at that time but may look obvious right now. In those days, the best computers adopted vacuum tubes to achieve the desired function. The first PLATO system used a TV set and a Teletype keyboard that was connected to the University's ILLIAC vacuum tube computer [9]. One of the key issues of this new graphics display invention was to have inherent memory so that the bulky and expensive scan converter tube memory could be eliminated. Fig. 2.2 shows an early plasma display as it was connected to the glass vacuum system used for the first generation. The first device used neon gas to generate the familiar neon orange glow.

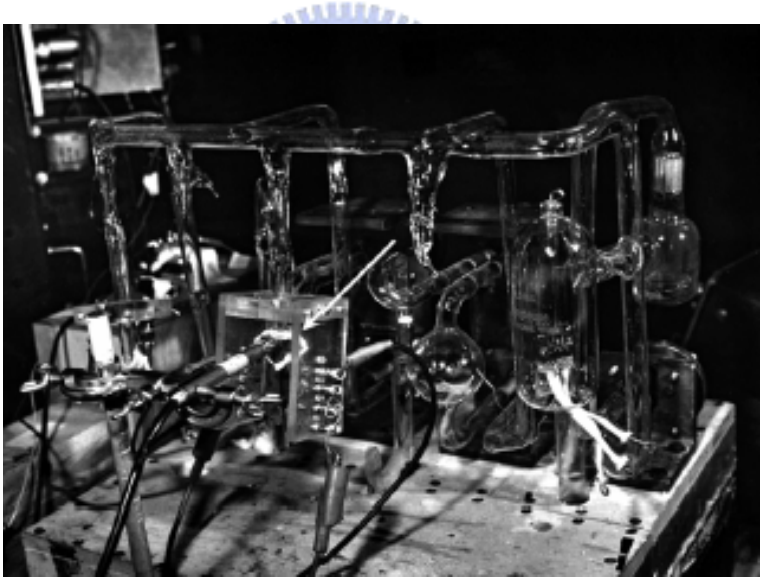

Fig. 2.2 Early plasma panel attached to the glass vacuum system at the University of Illinois. Arrow points to the 1-in by 1-in panel. This had the same alternating sustain voltage, neon gas, and dielectric glass insulated electrodes that have been widely used for PDP today [9].

Somehow, this vacuum system had a leak that a small amount of air would be added to the neon. The solution for this situation to prevent the leakage was to add a portion of a percent of nitrogen into the neon to achieve inherent memory.

The original monochrome panels were achieved and became popular in the early 70s. Then there followed a long period of sales decrease in the late 1970s as semiconductor memory made CRT displays relatively cheaper than plasma displays. However, IBM introduced a 19-inch monochrome display (orange on black) which was able to show four simultaneous 3270 virtual machine (VM) terminal sessions in 1983. And late in 1992, Fujitsu announced the world's first 21-inch full color plasma display panel. A hybrid based on the plasma display created at the University of Illinois at Urbana-Champaign and NHK STRL, achieves superior brightness and good image quality. In 1997, Pioneer started the business selling the first plasma television in the markets. At that time (1922), screen sizes can only achieve about 21 inches. Right now, the largest plasma display in the world shown at the CES (Consumer Electronics Show) in Las Vegas in 2006 made by Matsushita Electrical Industries (Panasonic) measured 103-inch.

Until quite recently the superior brightness and wider viewing angle, plasma display panels become one of the most popular forms of display for HDTV. However since that time improvements in LCD technology have closed the gap dramatically. The lower weight, price and power consumption of LCDs have seen them make large inroads into the former plasma market.

2.1.1 Invention of Plasma Display Panel

Back to the early stage of plasma display, Fig. 2.3 shows the details of the plasma display that appear in the original patent [10]. Basically, the fundamental concept was to insulate the driving electrodes with dielectric layers and located between the electrodes and the neon gas mixture contained in cells. Two main issues should be notified. First of all, this is a pretty practical way to limit the current of the gas discharge and prevent arcs. The dielectric layer could be deposited quite uniform and at low cost. Secondly, the dielectric layer could be used to store charge on the walls, a necessary requirement for the inherent memory feature. Each pixel could store its own isolated wall charge, which allows pixels to be in either the on or the off state even when placed along a external electrode.

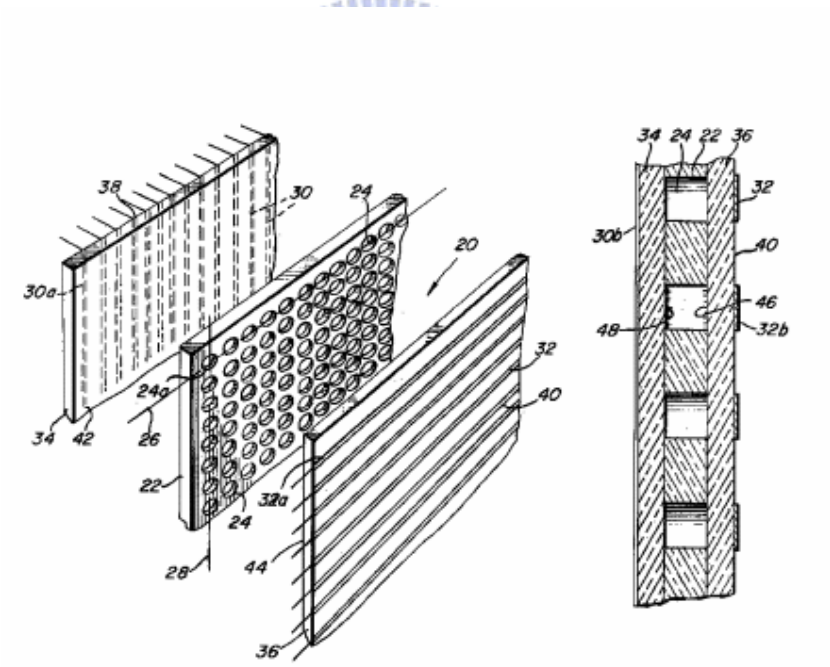

Fig. 2.3 The original drawings of plasma panel from the University of Illinois at Urbana Champaign (UIUC) [10].

Fig. 2.4 shows the first plasma panel with multiple pixels. This result was first published in 1966 [11]. This was a major achievement because it was also the panel

that demonstrated the first matrix addressability [12]. The image on the panel was selectively addressed using a write pulse applied through a resistor that biased the sustain voltage to the point where a discharge would occur. This is the first time that the inventor named this device the “Plasma Display Panel.”

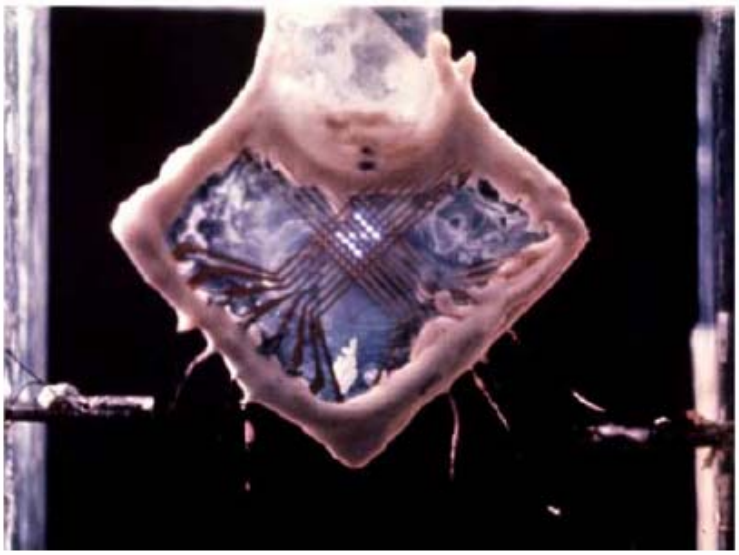

Fig. 2.4 Early 4 by 4 pixel panel presented in the first publication of the plasma display panel by University of Illinois in 1966. This panel was the first to have more than one pixel [11].

In 1967, another important achievement by the University of Illinois was to develop the first color plasma panel, which is shown in Fig. 2.5 [13]. The ultraviolet (UV) light generated by a xenon gas discharge to excite red and green phosphors was used in this project. There are three cells situated in this device, including one with a red phosphor, a green and a non-phosphor one. All plasma TVs produced today use the UV light from xenon gas discharge exciting the phosphors in the exact same way it was done by this early device.

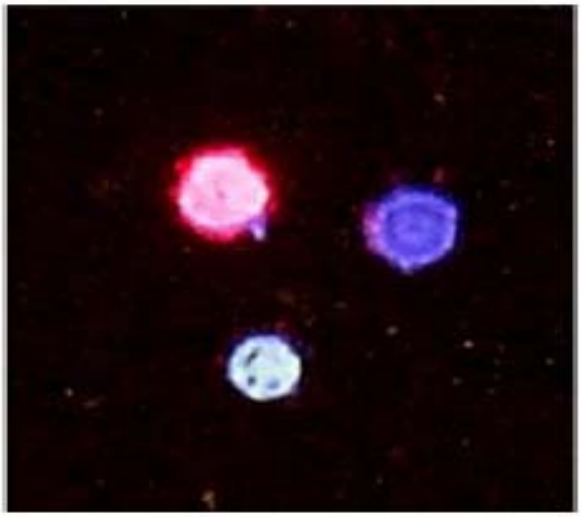

Fig. 2.5 First color plasma panel was this three cell prototype with red and green color phosphors excited by a xenon gas discharge. It was developed at the University of Illinois in 1967. All of today's color plasma TVs basically generate light in this way [13].

2.1.2 Practical Commercial Structure

Accordingly, the devices developed by the University of Illinois proved that the fundamental ideas are feasible, but they were still too fragile for public applications or commercial products. The original devices were made with three 150μm thick sheets which were commonly used for microscope cover slips. Very thin transparent gold electrodes were placed on the surface of the outer sheets, and the inner sheet had holes for each pixel, as shown on the right side of Fig. 2.6. On the other hand, torr-seal vacuum epoxy was adopted here to bond these three sheets together. One problem for this arrangement is that they could not be baked to a temperature much higher than 100˚C or the epoxy would decompose. As a result, leakage, breakage, and gas contamination became the biggest issues in this condition.

In 1968, some manufacturers developed the panel shown in Fig. 2.7 having the open-cell structure shown in Fig. 2.8. [14] This structure consists of two robust 6-mm-thick substrates made of soda-lime glass and could be fabricated in the mass

production line. The thick film electrodes made of gold with glass paste was screen printed and fired on each of the substrates and then coated with a 25 μm thick-film lead–oxide-based solder-glass dielectric layer. This device could be baked under vacuum at 350°C to drive out contaminants and then filled with an all inert penning gas mixture of Ne plus 0.1% Ar. This panel was strong and the gas remained pure.

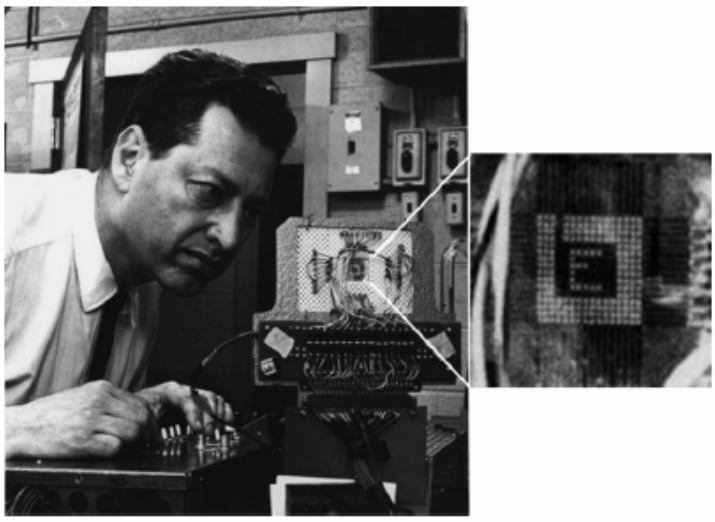

Fig. 2.6 Prof. H. Gene Slottow manually addressing a 16 by 16 pixel plasma panel, developed by University of Illinois in 1967. Magnified view on the right shows the very small 1-in by 1-in panel.

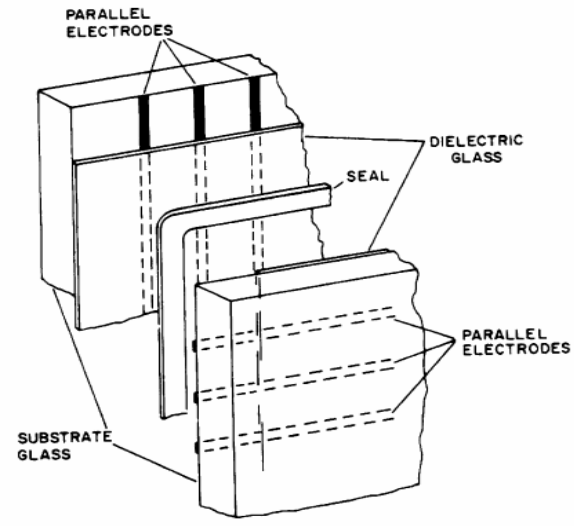

Fig. 2.7 Early open-cell structure developed by Owens-Illinois in 1968. The substrate glass was 6 mm thick and the dielectric glass layers were 25 μm thick [14].

Fig. 2.8 Open-cell structure was used in this 128 by 128 pixel plasma display developed by Owens Illinois in 1968 which measured 4-in by 4-in. It consisted of a robust 6-mm-thick glass substrate, thick film gold electrodes, and a screen printed solder glass dielectric layer [14].

Later in 1968, they developed a new type consisting of 100x100 mm area and an array of 128x128 pixels, as shown in Fig. 2.9. The front plate of this plasma display is a module for the modern PDPs. The front plate of today's PDPs has a fundamental structure very similar to that used for the front plate. After this very significant breakthrough, the University of Illinois continued to play an important role by teaching to the industry the art of electronic addressing and sustaining [15]. The plasma display received significant recognition when it won the prestigious IR-100 Award in 1968. The 16x16 pixel panel shown in is the most beautiful example of the old micro-sheet panels at that time.

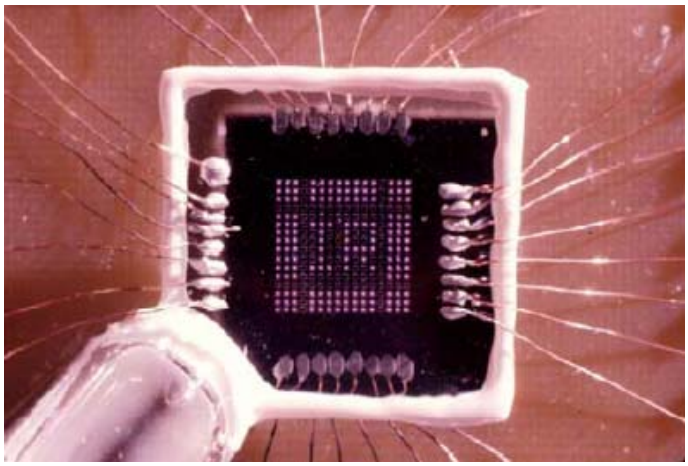

Fig. 2.9 16 by 16 pixel plasma display panel. The Industrial Research 100 Award was given to the University of Illinois in 1968 [15].

2.1.3 Key Features for TV Development

A. DC Plasma Displays

In the early days before PDP was invented, direct-current (DC) PDP operated by neon negative glow had been developed for the display application. The DC- PDP was invented by Burrough Co. in the early of 1970s [16]. In those days, they used a resister to limit the discharge current instead of the capacitor. DC-PDP had a dc discharge that acted like a shift register and addressed the individual pixels in the panel. It had lower circuit costs due to the reduced number of external panel electrodes. They also developed a dc plasma memory method that did not require resistors [17]. Later on, this had been used in many future prototype color displays. For many years until early 90s, there were existing two types of plasma displays. The type that used resistor current limiting became known as the DC-PDP. The original plasma display panel that used capacitor current limiting became known as the AC-PDP.

B. Grayscale

After successfully making plasma in the cell, how to create the desired image becomes the next topic. However, there comes a big problem for grayscale images because a pixel was either “on” or “off.” As a result, to make a half- on state becomes a critical issue. Unlike CRT using the electron gun to scan each line, PDP uses memory effect to gather wall charge for the ignition of plasma. The inherent memory of PDP has advantages for making bi-level graphic displays. By the memory eddect, PDP uses wall charge to decide the “on” or “off” state of each cell. In 1972, the grayscale problem was solved independently by Mitsubishi [18] and Hitachi. This used a technique of writing and erasing every pixel many times in a given frame so that a grayscale could be observed based on the amount of time the given pixel was on during the frame. This driving skill is well known as the Address While Display (AWD) method.

C. Full Color PDP

In 1978, NHK (Japanese Broadcast Corporation) as known as the most active group for DC-PDP revealed a high-quality full-color plasma TV panel with a 16 in diagonal [19]. After that, NHK continued the work and keep a major force in the development of color DC-PDP. This came as a natural consequence of their pioneering development of high-definition television (HDTV). NHK realized that high resolution image looked fantastic on a large screen because the visual acuity of the eye limits the ability to see high resolution on a small screen. For this reason, they believed that the large screen potential of the plasma display could solve this problem. However, even the future for color PDP looks very exciting in the mid 1970s, it takes more than two decades of research for the practical color PDP products to emerge.

2.2 Plasma and VUV Generation

In the following pages, the basic concept and working mechanism of the transformation from ionized gas to visible light would be introduced. PDP uses ionized gas discharge (plasma) to generate vacuum ultraviolet (VUV) to stimulate the phosphor layer. The stimulated red, green and blue phosphor layer would emit visible light though the front panel to the human eyes. Fig. 2. 10 shows the visible light emission process of plasma display panels.

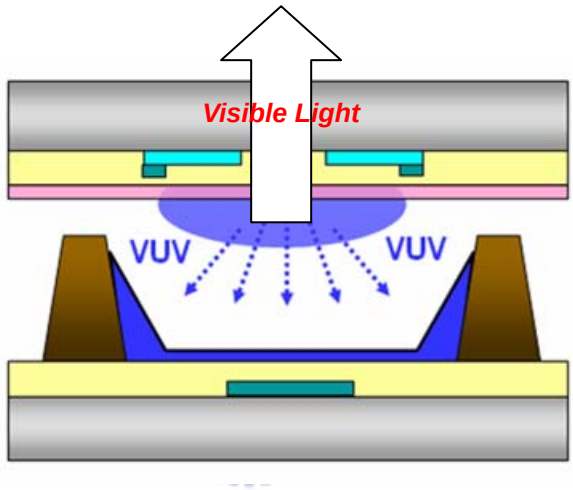

Fig. 2. 10 The visible light emission process of plasma display panels. VUV is generated by plasma and is going to stimulate the phosphor layer to emit visible light.

2.2.1 Principle of Plasma Physics

What is plasma? The central element in a fluorescent light is plasma. Plasma is known as the fourth state of matter in the universe besides solid, liquid and gas. Basically, a gas made up of free-flowing ions (electrically charged atoms) and electrons (negatively charged particles) is identified as plasma. As shown in Fig. 2. 11, under normal conditions, a gas is mainly made up of uncharged particles. That is, the individual gas atoms include equal numbers of positively charged particles and

electrons. The negatively charged electrons perfectly balance the positively charged protons, so the atom has a net charge of zero.

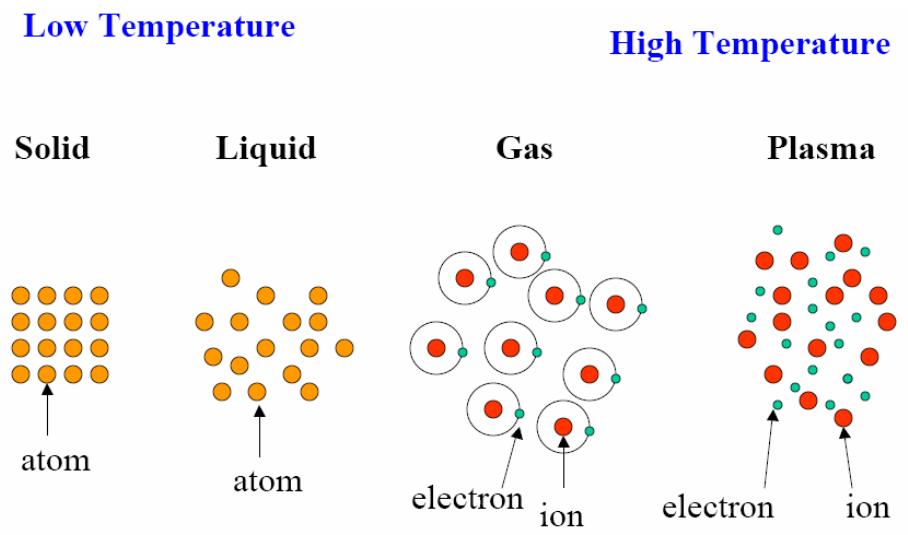

Fig. 2. 11 Plasma is recognized as the fourth state of the matter. Figure 2.11 shows the other three states in the universe includes of solid, liquid, and gas.

Plasma can be generated by introducing a lot of free electrons into the gas via establishing an electrical voltage across it. The free electrons collide with the atoms, knocking loose other electrons. With a missing electron, an atom loses its balance. It has a net positive charge, which makes it an ion. In the plasma with an electrical current running through, negatively charged particles are rushing toward the positively charged area of the plasma, and positively charged particles are rushing toward the negatively charged area. Under this circumstance, particles are constantly bumping into each other with a high frequency. These collisions excite the gas atoms into the plasma, causing them to release photons of energy. For example, xenon and neon atoms, the atoms which have been used in plasma displays release light photons when they are excited. In PDP's case, these atoms release ultraviolet light photons

(Fig. 2. 12), which are invisible to the human eye. But ultraviolet photons can be used to excite visible light photons by stimulating the phosphor layer.

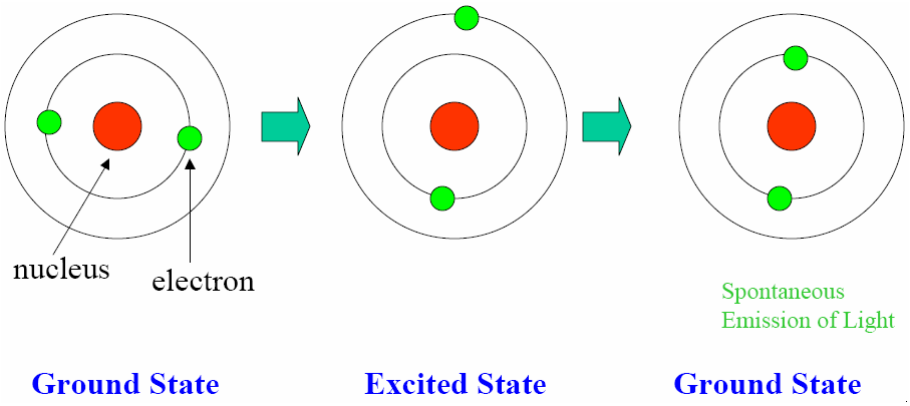

Fig. 2. 12 Where does the UV come from? Ultraviolet is emitted while a electron jumping back to the ground state of excited state.

2.2.2 Ionization and Gas Discharge

Unlike direct ionization, penning ionization is defined as the ionization that occurs through the interaction of two or more neutral gaseous species, at least one of which is internally excited. If A* denotes an excited electronic state of atom A and B the ground electronic state of another atom (or molecule), then the process

$$A^* + B \rightarrow A + B^+ + e^- \qquad (2a)$$

is known as *Penning ionization* (PI), and the related process

$$A^* + B \rightarrow (A\,B)^+ + e^- \qquad (2b)$$

is called *Associative ionization* (AI). Reactions of this type have long been considered by worker dealing with ionized plasmas, where order-of-magnitude estimates of rate coefficients have been sufficient for these purposes. If A* is metastable, however, it

may live long enough to be studied by molecular beam method [20].

Among those types of gas discharge, xenon and neon are the most popular gas adopted in the cells for plasma display panel. Taking Xe and Ne for example, the gas discharge process can be categorized into four parts, (I) The excitement and de-excitement of the electron impact; (II) The ionization and recombination of the electron impact; (III) Two-body heavy particle collisions; (IV) VUV radiation.

The Excitement and De-Excitement of the Electron Impact

$$Xe + e \rightarrow Xe^{*} + e \quad (2\text{-}1)$$

$$Ne + e \rightarrow Ne^{*} + e \quad (2\text{-}2)$$

$$Xe^{*} + e \rightarrow Xe + e \quad (2\text{-}3)$$

$$Ne^{*} + e \rightarrow Ne + e \quad (2\text{-}4)$$

The Ionization and Recombination of the Electron Impact

$$Xe + e \rightarrow Xe^{+} + e + e \quad (2\text{-}5)$$

$$Xe^{*} + e \rightarrow Xe^{+} + e + e \quad (2\text{-}6)$$

$$Xe_2^{*} + e \rightarrow Xe_2^{+} + e + e \quad (2\text{-}7)$$

$$Ne + e \rightarrow Ne^{+} + e + e \quad (2\text{-}5)$$

$$Ne^{*} + e \rightarrow Ne^{+} + e + e \quad (2\text{-}6)$$

$$Ne_2^{*} + e \rightarrow Ne_2^{+} + e + e \quad (2\text{-}7)$$

Two-Body Heavy Particle Collisions

$$Xe^{*} + Xe^{*} \rightarrow Xe^{+} + Xe + e \quad (2\text{-}8)$$

$$Ne^{*} + Ne^{*} \rightarrow Ne^{+} + Ne + e \quad (2\text{-}9)$$

$$Xe + Ne^{*} \rightarrow Xe^{*} + Ne \quad (2\text{-}10)$$

$$Xe + Ne^{*} \rightarrow Xe^{+} + Ne + e \quad (2\text{-}11)$$

2.2.3 Vacuum Ultraviolet (VUV)

As described in 2.2.2, based on the different ionization phenomenon, plasma display panel would be able to emit visible light by the gas discharge and VUV generation first [21].

VUV Radiation

$$Xe_2^* \rightarrow Xe + Xe + h\upsilon \qquad (2\text{-}12)$$

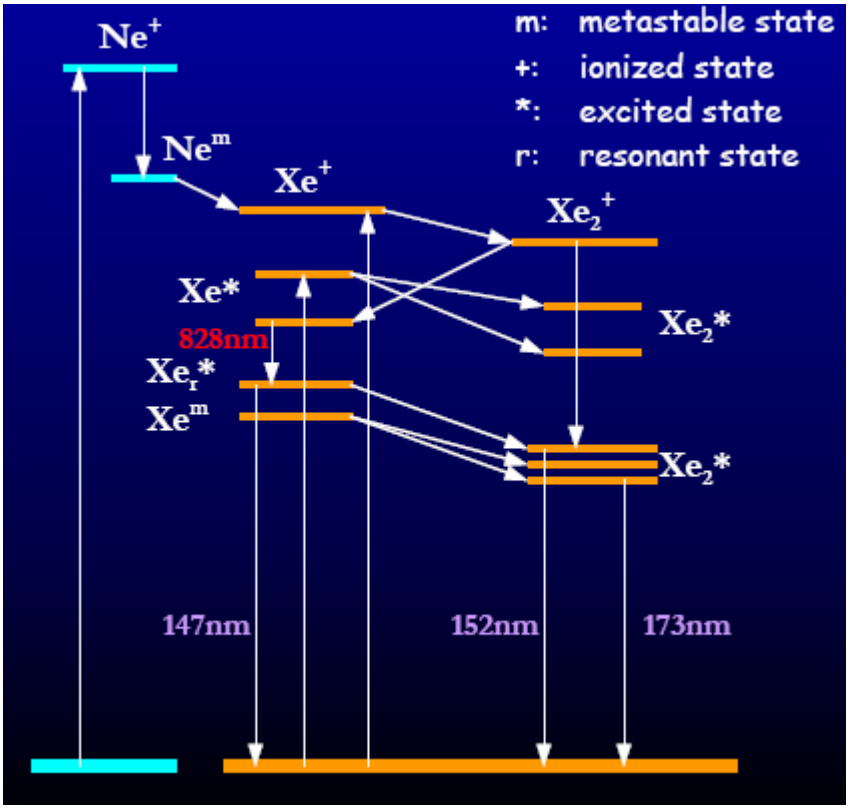

Fig. 2. 13 The energy level and states of xenon gas discharge. PDP uses 147 nm and 173 nm UV light to stimulate the phosphor laer.

PDP uses the excitation and emission of the particles by emitting 147nm, 152nm and 173 nm wave length to generate the ultraviolet (UV). The energy level and states of the gas discharge used in plasma display is illustrated in Fig. 2. 13. During the UV

transportation, around 30% of the energy transferred to the kinetic energy of electrons and the other 70% transferred to the kinetic energy of charged particles. Under acceleration of electric field, the average kinetic energy of charged particles can only reach to several electron volts due to its lighter weight compared to that of electron. This low kinetic energy of charge particle can not provide sufficient help for UV generation but transforming into heat loss. On the other hand, around 20% of the electron kinetic energy will transform into the UV light through inelastic collision. As a result, only 6% of the imported energy will be capable transformed into the UV light generation.

2.2.4 Photoluminescence

Photoluminescence is a process in which a chemical compound absorbs a photon with a wavelength in the range of visible electromagnetic radiation, transitioning to a higher electronic energy state, and then radiates a photon back out, returning to a lower energy state. The period between absorption and emission is typically extremely short, on the order of 10 nanoseconds. Under special circumstances, however, this period can be extended into minutes or hours.

Ultimately, available chemical energy states and allowed transitions between states (and therefore wavelengths of light preferentially absorbed and emitted) are determined by the rules of quantum mechanics. The simplest photoluminescence processes are resonant radiations, in which a photon of a particular wavelength is absorbed and an equivalent photon is immediately emitted. This process involves no significant internal energy transitions of the chemical substrate between absorption and emission and is extremely fast.

More interesting processes occur when the chemical substrate undergoes internal energy transitions before re-emitting the energy from the absorption event. The most

familiar such effect is fluorescence, which is also typically a fast process, but in which some of the original energy is dissipated so that the emitted light is of lower energy than that absorbed.

An even more specialized form of photoluminescence is phosphorescence, in which the energy from absorbed photons undergoes intersystem crossing into a state of higher spin multiplicity, usually a triplet state. Once the energy is trapped in the triplet state, transition back to the lower singlet energy states is quantum mechanically forbidden, meaning that it happens much more slowly than other transitions.

2.3 Driving Waveform

The most popular driving waveform goes to the address display separated (ADS) method proposed by a Japanese Company Shinoda [22]. The driving waveform used in one of the sub-fields is demonstrated in Fig. 2.14. With ADS driving method, cells are first erased by a reset step, then addressed (i.e. memory charges are deposited in the cells which need to be ON during this sub-field), and the addressed cells are turned ON during the sustain period because the previously generated wall charges in the address period served as priming seeds. The address and display periods are therefore clearly separated in the ADS method.

Moreover, the cells are addressed line by line. One voltage is applied to all the X electrodes. The reset period is used to erase space charges in the cell and set all the cells to the same initial state; the memory charges are first erased, afterward, all the cells are then turned ON with a write pulse, and then erased again. Memory charges are written on the cell when the scan pulse of a given Y electrode coincides with a pulse on the corresponding address electrode. After the cells of the whole screen have been addressed, sustain period launches and a discharge occurs in the cells which have been addressed, at a given subfield numbers.

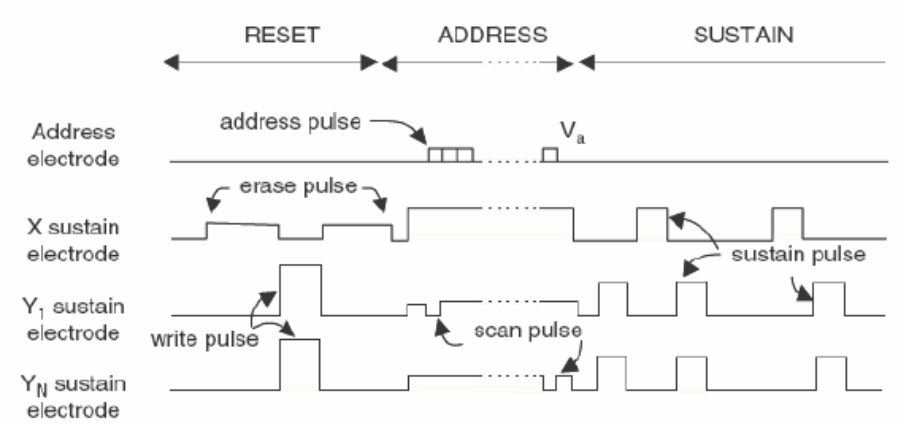

Fig. 2. 14 The most popular driving waveform — address display separated (ADS) method proposed by a Japanese Company Shinoda. Figure 2.14 shows the driving waveform used in one of the sub-fields

2.4 Protective Layer – MgO

Magnesium Oxide (MgO) is now fully adopted as a protective layer in the plasma display panel. It plays a very important role in the AC-plasma display panel (AC-PDP) to protect the electrode and the dielectric material from the bombardment of ions, electrons, photons, and metastable atoms.

The discharge voltage of an AC-PDP is largely affected by the protective layer since the operation mechanism of the plasma display panel is based on the gas discharge phenomenon occurring around the protective layer that covers the dielectric layer. In actual operation of PDP, a low firing voltage is required to conserve the electrical power of the driving circuit. When the AC pulse voltage is applied at some high frequency between the discharge electrodes, and the plasma is ignited in the gas volume, the protective layer plays a role in reducing the voltage for discharge by means of emitting secondary electrons. Thus, MgO has been used as a surface protective layer on the dielectric material in the AC-PDP. However, materials with

better electrical characteristics are needed to meet the demands of advanced high-vision PDPs with low-power consumption. Thus, many research groups have tried to make new protective materials with better electrical characteristics than MgO.

So far, many researches have been made for the development of high efficiency dielectric protection materials including Al_2O_3, La_2O_3 and CeO_2, and, it is known that MgO is the best candidate for the dielectric protection material. Unique features such as high secondary electron emission coefficient (γ), high transparency, and good sputtering resistance are the main reasons that give MgO such a big success till now. Bulk magnesium oxide is known as a highly ionic crystal with the Mg—O bonds having about 80% ionic character. Generally, ionic materials have the strong bonding. The electron induced secondary electron emission coefficient of the evaporated magnesium oxide is as high as 17, much higher compared with that of Al_2O_3, a value of 3.2 [23].

In this section, MgO as a protective layer evaporated by electron beam induced would be introduced in detail including development of PFP history, chemical profile, physical characteristics, and TV application.

2.4.1 MgO development in PDP History

In the early days, the original open cell structure was not yet optimized for the display application even though it was already very practical. The dielectric layer was not a very suitable gas discharge cathode because the very energetic ions in the cathode fall would sputter the surface and erode the surface structure. This defect on the surface may result in the decrease of secondary electron emission coefficient (γ), unstable discharge and varied driving and sustaining voltage. Such a voltage drift was unbearable in the display application where one sustain voltage needed to be adjusted for all the other million pixels. Unfortunately, the voltage of the on-state pixels would

drift at a different rate than the pixels that were at off-state. The remarkable breakthrough came in 1971 with the development of the MgO protection layer cathode.

After the dielectric layer was deposited, a 500-nm-thick layer of MgO was deposited by electron beam evaporator on both the front and rear panel. Electron beam evaporation also becomes the general method to evaporate MgO thin film on dielectric layer in modern PDPs. This refractory magnesium oxide helped the voltage condition became quite stable in the life test. The key features consist of very high ion-induced secondary electron emission and a very low sustain voltage. It was believed that the MgO protective layer for plasma displays was independently invented at three different companies: IBM, Owens-Illinois, and Fujitsu [24]. The first PDP products with MgO were developed in October of 1973 by IBM. [25]. Arguments were made in U.S. courts for many years in order to decide which company invented MgO for the plasma display application. Ultimately, the courts awarded the MgO patent to Owens-Illinois.

2.4.2 Chemical and Physical Profile

Magnesium is a silvery white metal. The surface of magnesium metal is covered with a thin layer of oxide that helps protect the metal from attack by air. Once ignited, magnesium metal burns in air with a characteristic blinding bright white flame to give a mixture of white magnesium oxide, MgO, and magnesium nitride, Mg_3N_2. Magnesium oxide is more normally made by heating magnesium carbonate. Calcium, immediately below magnesium in the periodic table is more reactive with air than magnesium.

$$2Mg(s) + O_2(g) \rightarrow 2MgO(s) \quad (2\text{-}12)$$

$$3Mg(s) + N_2(g) \rightarrow Mg_3N_2(s) \quad (2\text{-}13)$$

Magnesium oxide has an empirical formula of MgO. It is a white solid mineral that occurs naturally as periclase and is a source of magnesium. Periclase is sometimes used as a gemstone although it lacks good hardness and is generally limited in colors. Periclase is relatively scarce and is found in marbles being formed from the dissolution of dolomite, $CaMg(CO3)2$, into MgO-periclase, $CaCO_3$ and CO_2.

MgO is widely used as a sport for absorption and growth of different materials, such as metals, semiconductors, superconductors and optoelectronic devices. It is also used as a catalyst for heterogeneous reactions. It is formed by an ionic bond between one magnesium atom and one oxygen atom. MgO (sometimes called magnesia) is formed commercially by heating magnesite to 600－800 ˚C, which drives off most of the CO_2. It has good thermal conductivity and electrical resistivity at elevated temperatures. Following catalogs the general description of MgO:

Magnesite — A mineral composed of $MgCo_3$.

Magnesite Grain — dead-burned magnesia in granular form in size suitable for refractory purposes.

Seawater Magnesite — Dead-burned magnesia made by a chemical process using seawater or other solutions (brines).

Periclase — The high temperature form of magnesia.

Table 2.1 shows the fundamental chemical and physical properties of MgO. Usually MgO is composed of single crystals, pieces, targets, and powder sized as fine as nanometers. The theoretical composition of magnesite is around: MgO= 47.8% and Co_2= 52.2%.

Table 2.1 The chemical and physical profile of MgO.

Appearance	White, Powdery, Solid
Molecular Weight	40.3 g/mol
Melting Point	3073 K (2800 ˚C)
Boiling Point	3873 K (3600 ˚C)
Bulk Density	3.58 g/cm^3
Crystal Structure	Cubic FCC
Lattice Constant	a=4.13 Å

2.5 Summary

The introduction to PDP history and fundamental working mechanism are introduced in this Chapter. Literature surveys point out the key features and state the critical issues of plasma display panels. Among those features and characteristics, MgO thin film as a protective layer is considered as one of the most important issues. In the following chapter, experimental setup will be designed to modify the effect of MgO thin film on PDP performance. E-Beam evaporation would be adopted to deposit the MgO thin film on the dielectric layer. Flow of fabrication process would also be introduced in Chapter 3.

Chapter 3

Fabrication and Measurement Instrument

Plasma display panels (PDPs) can be made in large sizes and are expected to be the best candidates for wall-mount displays that are too big to be made using CRTs (i.e., 40-inch and larger). However, broadcasting of high-definition TV (HDTV) will start when digital TV broadcasting begins, and resolutions exceeding one million pixels will be required even for standard TV units.

3.1 Introduction

The markets for large area PDPs larger than 40 inch diagonal size have been expanded rapidly. The large area flat panel display is demanded for a HDTV and a digital TV which displays a real and life-size image in addition to the traditional TV image because of the development of the both computer and network technologies. This propagation includes the three-color PDP in 1989, the 21-inch diagonal color PDP with 260 thousand colors in 1993, and the 42 inch diagonal full color PDP with 16.7 million colors in 1996. These results have opened the dream of a wall hanging TV. Looking back a history of color PDP, a development of the 21 inch PDP was the most important step in which the most essential technologies for large area PDPs have been completed. The commercialized 42 inch and 50 inch PDPs have been developed based on several technologies [26–29]. This chapter will describe the manufacturing technologies for modern color PDPs in the markets.

Before introducing the flow of PDP fabrication process, fundamental PDP structure would be reviewed firstly. The practically developed T-shaped PDP structure is shown in Fig. 3.1. Paired parallel display data electrodes, sustain electrode

X and scan electrode Y, are formed on the front glass substrate. Each display electrode is composed of a transparent SnO_2 (ITO) and a narrow bus electrode of multi-layered Cr, Cu and Cr. They are capable to emit a luminance effectively through the transparent electrode and reduce the electrode resistance. These electrodes are covered with a dielectric layer which is made of low melting glass materials. This layer is covered by another protective layer－MgO thin film. Besides, striped address electrodes A are arranged on the rear substrate.

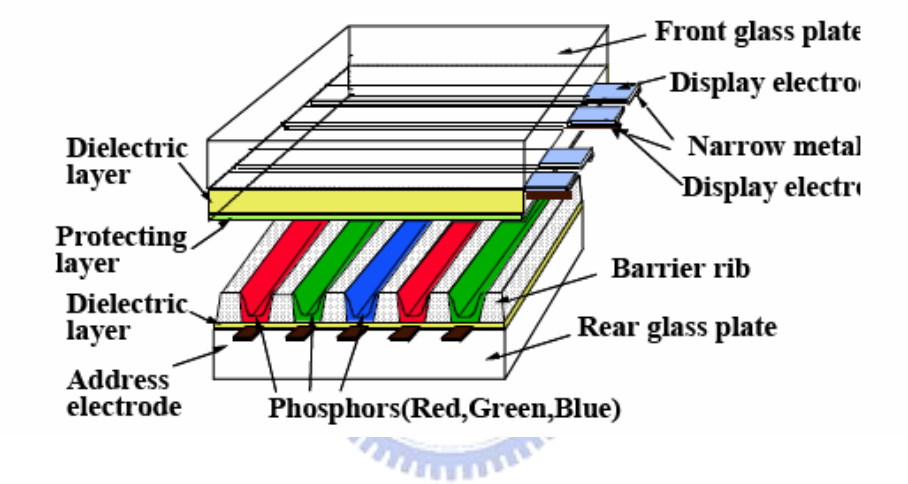

Fig. 3.1 The typical T-shaped structure which has been widely used in PDP products.

Striped type barrier ribs are on both side of the address electrodes to separate the adjacent discharge cells and to eliminate the optical cross-talk between each cell. Three primary color phosphor materials for red, blue, and green colors are deposited in the neighboring channels made by the ribs to cover both of the side wall of the ribs and the dielectric layer. The structure has realized good performances such as a high luminance, a high luminous efficiency and a wide viewing angle.

Phosphor materials are $BaMgAl1_4O_{23}$:Eu for blue, $(Y.Ga)BO_3$:Eu for red , and Zn_2SiO_4: Mn for green. The substrates are assembled onto each other with about 120

μm gap. A Ne + Xe gas mixture is introduced between the cell gap. The fabrication process is also simple enough to mass-produce so the PDP has advantages such as a low cost process and easiness to manufacture large area panels and high resolution panels.

3.2 Fabrication Process of Plasma Display Panel

Figure 3.2 shows the basic PDP fabrication process flow chart. First of all, the front plate process would be introduced. The transparent conductive ITO film is deposited onto the front glass panel. The multiple paired data electrodes are deposited by photolithography technology. As shown in the figure, the metal electrode film consists of a Cr/Cu/Cr multi-layer is sputtered on these transparent ITO electrodes. The bus electrode is also formed by photolithography technology. Besides, these electrodes are covered by a frit glass layer with screen printing method and then fired to about 600° C to turn out the dielectric layer. The seal glass layer with a width of about 3 mm is adhesive surrounded outside the display area with a pre-firing process. Additionally, MgO protective layer is evaporated on the dielectric layer over the display area of inside of the seal layer.

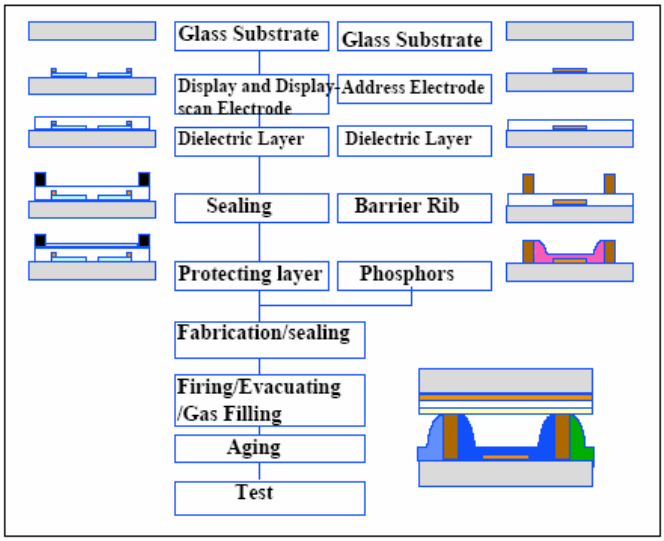

Fig. 3.2 The basic fabrication process of plasma display panel [30].

Following are the rear plate fabrication processes. A small hole of a diameter of about 1 mm is drilled on a corner of the rear plate. The Ag address electrodes are printed and fired. The frit glass is printed on the electrodes in the display area and then fired about 600° C to form the dielectric layer. The barrier ribs are made by sandblasting the frit glass on both sides of the address electrodes and then fire. The red, green, and blue phosphors are printed inside of the channel between the barrier ribs. Each color phosphors are printed simultaneously and repeated three times, and then dried. The rear plate is completed with these processes.

Both front and rear plates are assembled and fixed with clips. The assembled plates are fired to melt the seal layer and the plates are glued to integrate the panel. For the gas filling process, the panel is connected to an evacuation gas-filling system through the evacuating glass tube. After the baking step, the discharge gas mixture is then filled in. Finally, the whole PDP fabrication is completed after cutting off the evacuating tube. The driving pulse is applied to the panel and discharges are ignited in every discharge cells to reduce and make stable the operating voltage, which is known as the aging process.

3.2.1 Front Plate Fabrication

I. Glass Substrate

The most famous glass substrate company in PDP business goes to Asahi Glass Co., Ltd. It is reported that the number of PDP television sets is forecast to rise to 9 million units in 2007 from 1.4 million units in 2003, demonstrating annual growth of 60% during this period.

Asahi Glass started its PDP glass substrate production in 1996 at the Kansai Plant, becoming the world's pioneer in the field, and since then the Company's PD200 model has become a de facto standard. The PD200 now accounts for 90% of the

global market for PDP glass substrate products. This glass substrate material for PDP has been developed to prevent the distortion and the shrinkage of the glass substrate in the firing processes of high temperature. The high strain point glass has about 100° C higher strain point comparing to the conventional soda-lime glass. This eliminated the distortion and reduced the shrinkage in the process and then made it possible to construct the process with a large process margin.

II. ITO Electrode

The ITO (Indium Tin Oxide) or SnO_2 is designed for the use in AC-PDP. It is used for a transparent electrode in the front panel in order not to block the light transmission. ITO has excellent conductivity and good transparency but worse heat and etching resistance. Fig. 3.3 illustrates the processes for ITO and SnO_2 formation in the front panel fabrication.

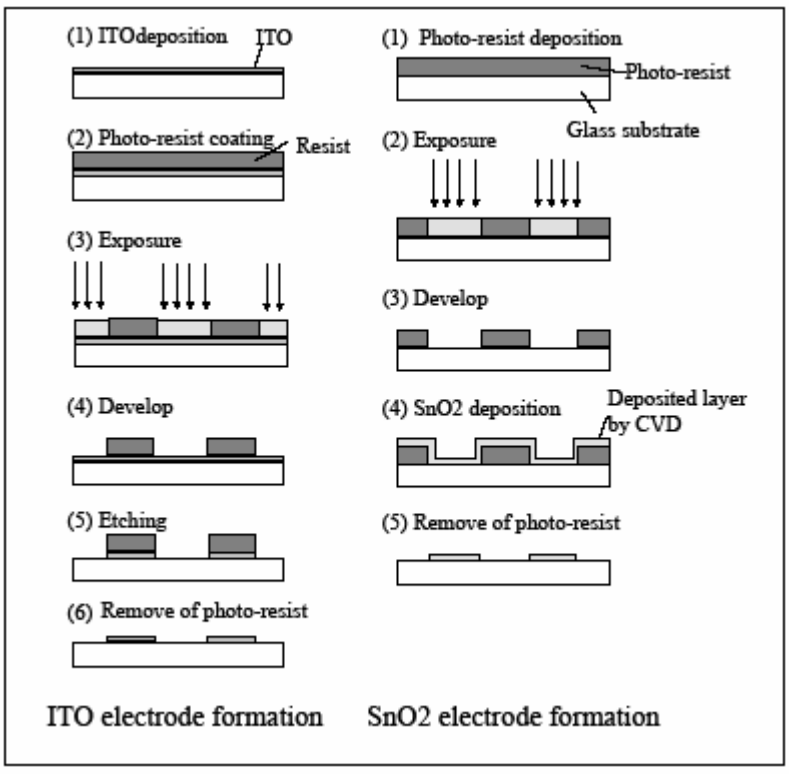

Fig. 3.3 Processes for ITO and SnO_2 formation in the front panel fabrication [30].

The ITO film is made by a sputtering or an ion- plating method. It is patterned by photolithography processes. A photo resist is usually coated with a roll-coating machine because of it's the large area. The expose uses a proximity method with a vertically supporting mechanics to prevent the bending of the glass substrate. As an exchange of a large photo mask is also a big issue, so the direct exposure machine is developed and practically used. The ITO film is etched with a solution of hydrochloric acid with small amount of nitric acid. The performances of the conductivity, transparency, etching ability, the adherence with Cr, resistance to the etching solution of Cr and resistance to the reaction with the dielectric layer while firing should be concerned to optimize an ITO films. Although SnO_2 has advantages on the stability of the film quality and conductivity over ITO, the etching parameters and conditions are too difficult to control. The film is now patterned with the liftoff process with heat resistant photo -resist.

III. Bus Electrode

Bus electrode is also known as auxiliary electrode. Since alarming heat would be released during the gas discharge and lead to the increasing resistance of transparent electrode, bus electrode is used to reduce the electric resistance of the transparent display electrodes. Ag and Cr/Cu/Cr are currently used to be the bus electrode. An Ag electrode is made with a printing method or a photolithography with photosensitive paste including Ag and frit glass as shown in Fig. 3.4. The Cr/Cu/Cr is made with sputtering method and patterned with photolithography method. Bus electrode is contributive to control and stabilize the gas discharge and enhance the conductivity, so it is considered as an auxiliary electrode.

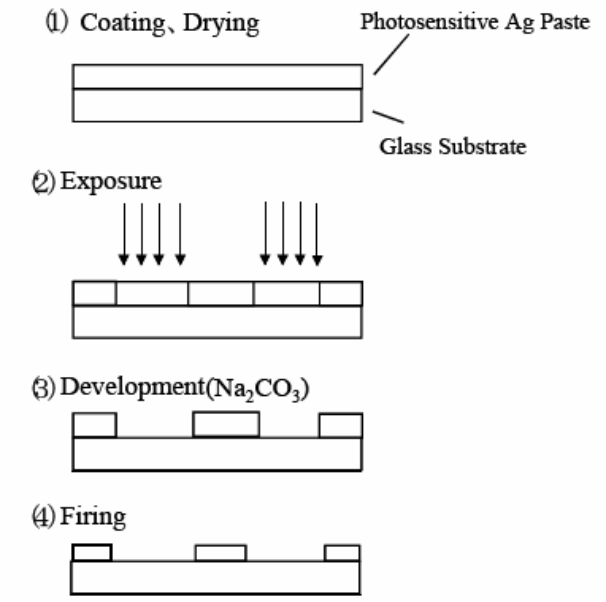

Fig. 3.4 An Ag electrode is made with a printing method or a photolithography process with photosensitive paste including Ag and frit glass [30].

IV. Dielectric Layer

Dielectric layer has good voltage resistance and is able to capture charges to achieve the memory effect. Dielectric layer is made by forming the layer of the low melting frit glass composed of and then fired at about 600° C to make transparent glass layer. It is important to make a uniform dielectric layer in the PDP fabrication process. The dielectric layer of a front substrate should have high transparency due to affect to the display performance. There are some methods to make the frit glass layer, such as screen-printing, slot coating, roll coating, and green sheet [30]. The most common method is screen-printing and shown in Fig. 3.5.

The glass layer is made by the way that the paste including frit glass and organic solution is deposited on the substrate through the mesh of screen. It is important to keep a sufficient time for leveling after printing to eliminate the roughness due to the mesh because the thickness uniformity affects on the differences in the discharge voltage of the cells. Beside screen printing method, two technologies are introduced. The slot coating method is the way that the glass paste is deposited through the slot of

thickness around 10 μm. The roll coating method is the way that once the layer of a paste is made on the roll and then transcribed on the substrate. Both methods do not use the screen mesh. There however remains an issue of that if the drying condition is controlled insufficiently, the uniformity is not adequate and the crack of the layer appears. The green sheet method is the way that a dried layer made on the base film is put on the substrate and then fired. Although this also realizes a good uniformity, a sufficient degas while firing is required because much organic binder is included in the glass film.

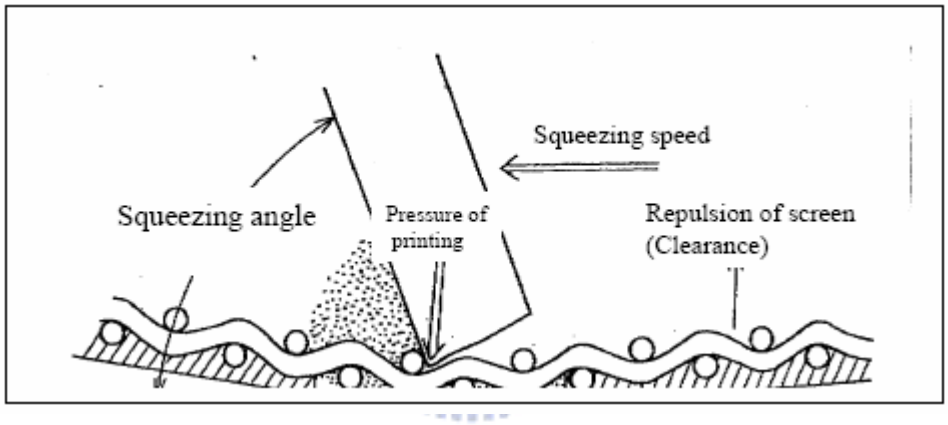

Fig. 3.5 Screen printing method [30].

V. MgO Protective Layer

It is believed that the protective layer is the one of the most key element to realize a good performance. At the early stage of PDP development, even though a lot of materials were investigated for the protection function, but MgO was then found to be the most appropriate material for a protecting layer [31]. Other materials were never successful because MgO combines several unique characteristics. The performances requested for the protecting layer includes high secondary electron emission, high sputtering resistance, high transparency, non-conductivity, high stability in the PDP fabrication processes

As a result, MgO becomes the most appropriate materials for these requirements. For the mass production, MgO layer is usually formed by electron beam evaporation method. E-beam evaporation can provide stable result and the cost is quite acceptable. There are several new methods have been investigated in order to achieve more efficiently production, such as ion plating, reactive sputtering, plasma treatment, etc.

3.2.2 Rear Plate Fabrication

I. Address Electrode

The address electrode process is almost same as the bus electrode in the front plate process. Since address electrode is located in the rear plate, there is no need to be transparent. Ag is currently adopted for the address electrode material. An Ag electrode is made with a printing method or a photolithography with photosensitive paste including Ag and frit glass. Just like bus electrode, address electrode is contributive to control and stabilize the gas discharge and enhance the conductivity.

II. Barrier Ribs

Barrier ribs are arranged and located to a spacer supporting front panel and separating each cell. The formation of barrier rib is one of the most unique processes in PDP fabrication and significantly effect could be seen on the cost. The thickness and width of the rib is around 150 μm and 70 μm, respectively. Although the printing technologies were used at first to make barrier ribs, the sandblasting method then took over due to the accuracy formation and excellent structure shape.

The sandblasting has advantage to get the high accurate barrier rib due to use the photolithography. Fig. 3.6 shows the process for sandblasting method. A thick frit glass layer is formed on the display area, and then covered with a dry photo-sensitive elastic film. The film is exposed through the film with barrier rib pattern and then

developed. The small hard particles are then sprayed out in a high pressure. Even though the frit glass layer of the area without elastic layer is cut, the area of the layer coated by the elastic film is remained because the particles would be reflected.

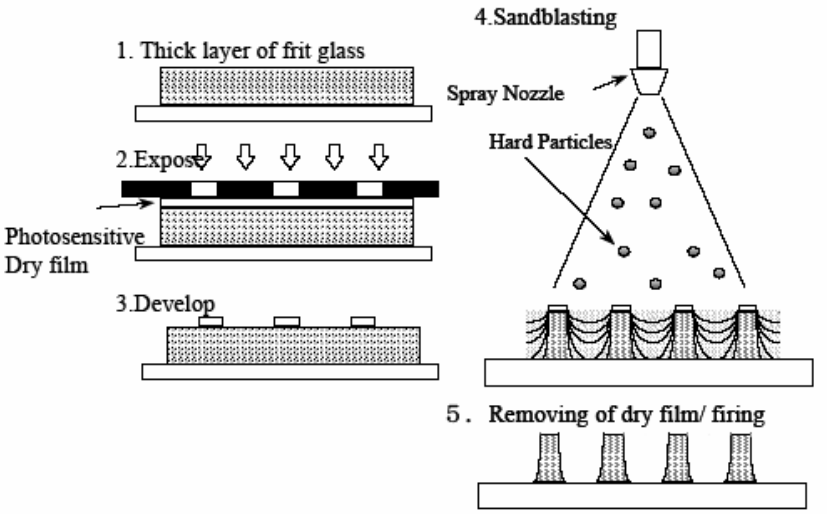

Fig. 3.6 Typically sandblasting method used to form the barrier ribs [30].

As shown in Fig. 3.6, the covered film is removed and then fired to complete the barrier ribs. The subject of the sandblasting process is that the 70 % of the materials formed on the plate are thrown away finally and then material cost is expensive. The recycle system of the material should be developed. In the photosensitive paste (PS) method, the thick PS layer composed of photosensitive material and frit glass is used. As the glasses in the PS layers reflect and disturb to make accurate barrier rib, thick layer is not possible at once. The processes of formation of PS layer and exposition are repeated two or three times and then fired to form the barrier rib.

III. Phosphor Layer

While depositing phosphor on the barrier ribs, it is important to prevent the cross printing. The printing method for phosphor layers is shown in Fig. 3.7. It is the most practical and efficient method so far in the industry. The phosphor formation process is unique because the phosphor layer is deposited on the barrier ribs and sidewall inside of the channel. The required tolerance of the phosphor deposition with the printing is not severe comparing to the printing processes for electrodes and barrier rib. That is because that as the phosphor paste is filled in the channel through the screen, the pattern of the screen can be designed narrower than the channel width. The filled paste is then dried. The drying condition is important to make uniform phosphor layers. The thickness of the phosphors can be determined by the composition of the phosphors in the paste. The phosphor layer deposited is shown in Fig. 3.8.

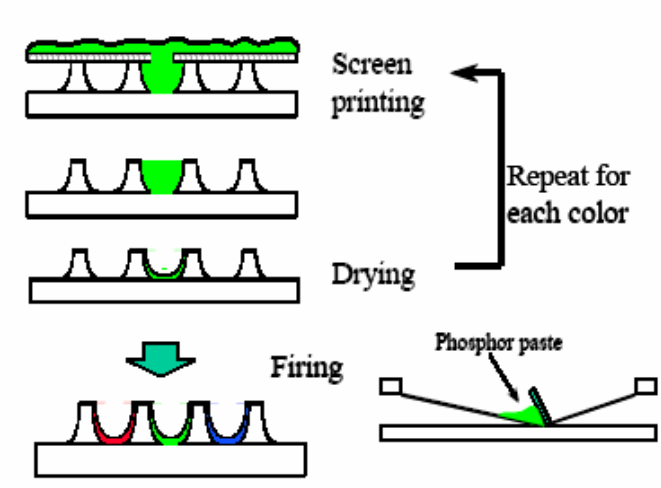

Fig. 3.7 Screen printing method used to deposit phosphor layer on the barrier ribs [30].

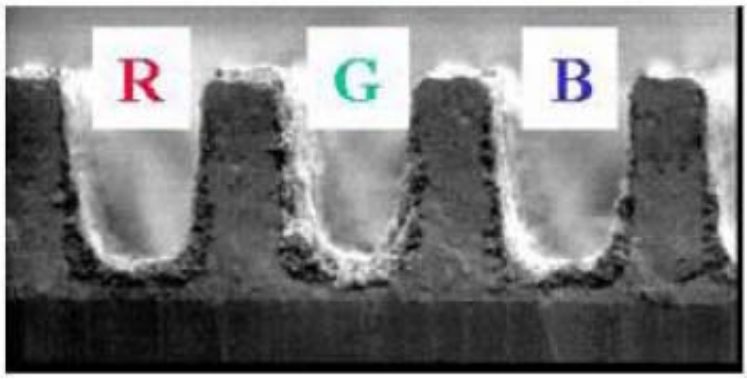

Fig. 3.8 Phosphor layer on the barrier ribs with red, green, and blue color [30].

3.2.3 Panel Assembling

After the front and rear panel process, it needs assembling, evacuation and gas filling to complete the whole fabrication process. The front and rear plates are assembled to align the display electrodes and address electrode in orthogonal. As shown in Fig. 3.9, the plates are pre-fixed with clips. The evacuating tube is placed on the hole with the frit paste and PCB. After the assembling, it is fired about 400° C to glue the plate each other by melting the seal layer. The panel is connected with an evacuation and gas filling system through the evacuating tube. The panel is placed inside of the furnace and baked out about at 350° C to evacuate the adsorbed gases on the surface of MgO, phosphors, barrier ribs and dielectric layers. After the sufficient baking, the panel is cooled down to the room temperature and then discharge gas is introduced to the designed pressure. Finally, the PDP is completed after cutting off the evacuating tube. As this process is one of the most important processes to decide the characteristics of PDP, the temperature while evacuation, evacuation system without impurity, and purity of filling gas should be controlled carefully. After the assembling, aging test is required to stabilize the panel discharge condition in order to provide normalized panel performance.

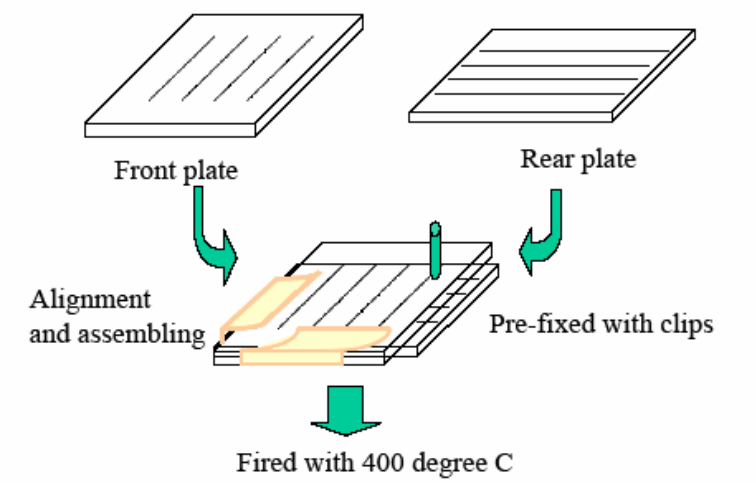

Fig. 3.9 Assembling process of front panel and rear panel. It needs to fire up to 400 degree C to seal the panel [30].

3.3 Experimental Setup

It is believed that PDP performance is strongly influenced by the surface characteristics of MgO thin films because the film is exposed to the plasma directly. Gas discharge and ion bombardment would sputter the surface structure and affect the panel properties. In this study, the deposition parameters are optimized and the relationship between the density of the MgO films and the properties of the AC-PDP is investigated. The influence of MgO density and surface morphology on panel properties has been examined with a accelerated life aging test.

The experiments in this study have been carried out to characterize the properties of twelve, 46-inch WVGA type plasma display panels. In order to characterize the effect of MgO thin film on PDP panel performance, several parameters would be chosen to make different formation MgO thin films. The experimental PDP modules are fabricated by ChungHwa Picture Tube (CPT) Co.

Table 3.1 The evaporation parameter of MgO thin film by E-Beam evaporation in this study.

No	O_2 flow rate(sccm)	Beam current (mA)	Thickness (designed)	Thickness (real)	C/V (deposition rate)	pressure
1	40	600	5000	5406	134mm/min	3.2×10^{-2}pa
2	50	600	7500	7717	95mm/min	3.1×10^{-2}pa
3	40	600	10000	9852	85mm/min	3.3×10^{-2}pa
4	40	650	7500	7605	140mm/min	3.1×10^{-2}pa
5	40	550	7500	7632	85mm/min	3.2×10^{-2}pa
6	10	600	7500	7452	126mm/min	1.2×10^{-2}pa

MgO thin film as a protective layer in experimental PDP modules were deposited by electron beam evaporation. The deposition parameters are categorized in Table 3.1. The MgO films were deposited at one of several value of O_2 flow rates (10, 40, 50

sccm), and electron beam current (550, 600, 650 mA). Moreover, different film thickness (5000, 7500, 10000 Å) were selected to examine the experiments and the temperature in the chamber during the evaporation is controlled from 220 to 240˚C.

After the panel fabrication, the bonding process required to attach the specific driving circuits on the back of rear panel. Afterward, each experimental PDP module was operated in an accelerated aging environment. In this study, the aging process requires a frequency three times higher than the conventional driving waveform and all of the panels were operated continuously prolonged to 1500 hours for the data recording.

Generally, the conventional PDP manufactured by CPT uses 40 sccm O_2 flow rate and 600 mA electron beam current to form a 7500 nm thick MgO thin film. Accordingly, the evaporated parameters were designed to investigate the details and panel properties difference between conventional ones and experimental ones. It is believed that varied oxygen flow rate during the Mg and O atom formation can change the stoichiometery of the MgO thin films [32–34]. We believe that this change can be a very key rule to the panel performance. Unlike bulk MgO, MgO thin films formed with different evaporation condition can also provide different thin film density, which is also a key element to affect the panel properties. Additionally, the change of evaporation parameters can also influence the surface morphology of MgO thin film. By the atomic force microscopy (AFM), surface morphology of MgO thin film would be characterized. Another thing to affect the MgO performance is the crystallinity of the thin film. Stronger crystal structure may guarantee lower sputtering rate against the ion bombardment. Therefore, X-ray diffraction (XRD) would be adopted to investigate the crystallinity of MgO thin films. All the detail experimental setup will be introduced in the next paragraph.

3.4 Measurement System

Figure 3.10 shows a 46-inch WVGA type AC-PDP module with the bonding driving circuits which has been used in this study. These experimental PDP modules consist of several innovating technologies for the color and driving including color rendering and color conversion (NTSC, EBU), de-contouring, dynamic white balance compensation, Gamma correction, lower level contouring technologies, etc.

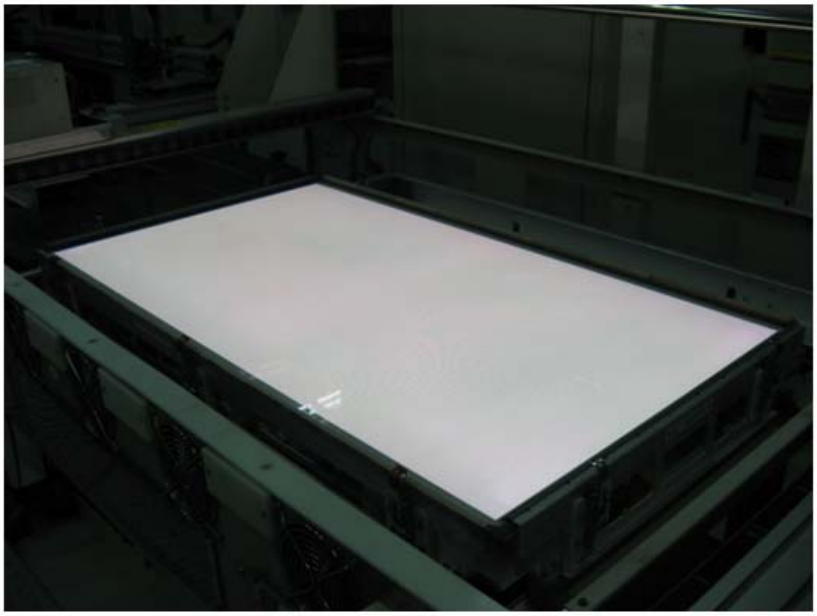

Fig. 3.10 The experimental PDP module with bonding circuits used in this study. It displays a full white 255 gray level in the figure.

Figure 3.11 illustrates the optical measurement system in this study. To light up the panel, red, green, and blue color patterns were generated by a pattern generator Axtro-828. By changing the program, desired color patterns can be demonstrated for the experiment request. It shows the different gray level patterns spread out bit by bit vertically in Fig. 3.12.

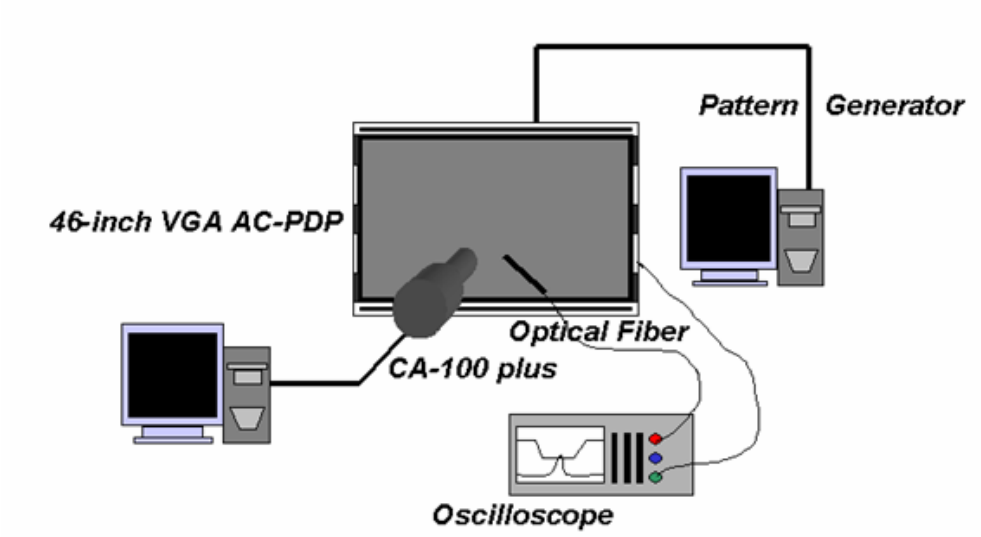

Fig. 3.11 The optical measurement system used in this study includes of photo diode, optical fiber, pattern generator Axtro 828, color analyzer CA-100, and oscilloscope, etc.

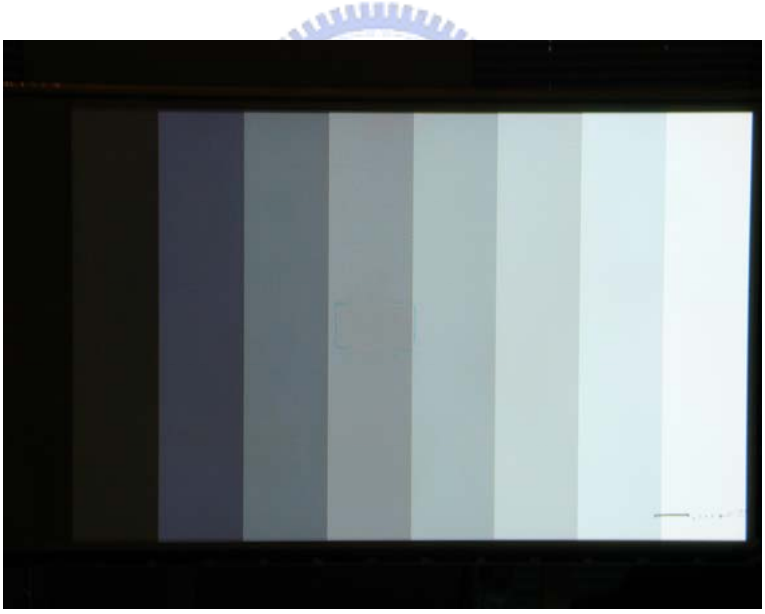

Fig. 3.12 The image shows the different gray level patterns spread out bit by bit vertically generated by axtro 828..

Key properties of each panel, including luminance, color temperature and CIE color coordinates of selected color patterns, were investigated with the color analyzer CA-100 as shown in Fig. 3.13. The sensor can measure and record the luminance (Y)

of the selected area by the contact. It can also modify the color temperature and point out the color coordinate (x and y) on the CIE chromaticity diagram. This system offers more precision in color measurement than do the Munsell and Ostwald systems because the parameters are based on the spectral power distribution (SPD) of the light emitted from a colored object and are factored by sensitivity curves which have been measured for the human eye.

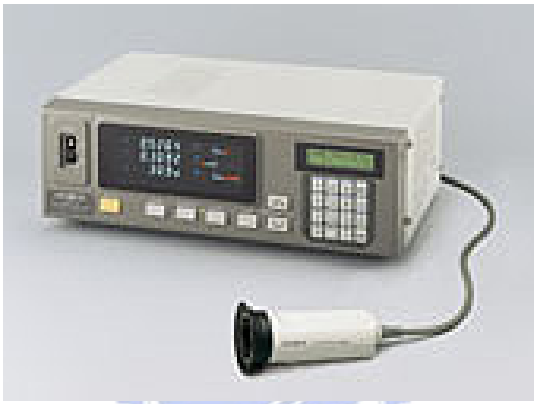

Fig. 3.13 Color analyzer CA-100 used in this work. Panel performance such as luminance, color temperature, color coordinate can be measured by this apparatus.

Measurements of the discharge lag were made with a photo diode, an optical fiber and an oscilloscope as shown in Fig. 3.14. We evaluated response time of discharge to writing pulse by measuring optical light emission. Fig. 3.11 shows the measuring system of light emission in terms of writing pulse. In measuring the characteristics of each panel the driving parameters were 70V, 2.8 μs writing (scan) pulse and a 180V sustaining voltage. To avoid effects of priming particles, all cells above the measuring line should be turn off with a full white 255 gray level. Light emission of the white cell was measured with respect to time of the writing pulse applied.

For the image sticking observation, CA-100 is used to record the luminance

degradation of the image sticking cells and the normal operated ones. In order to inspect the recover ability from the image sticking of different panels, panel performance such as luminance degradation and color coordinate variation of bright and dark backgrounds were investigated and recorded as a function of time. For the image sticking phenomenon observation, a full white 255 gray level square pattern is displayed in the center of the panel. The pattern is maintained continuously for 30 minutes and the luminance degradation is recorded as a function of operation time in order to make sure the discharge condition is stable for the observation.

Surface morphology and crystal structure of MgO are analyzed by atomic force microscopy (AFM) and X-Ray diffraction (XRD), respectively. AFM images would be used to characterize the surface condition of the MgO thin film while XRD techniques used to characterize thin film reflection geometry and crystallinity.

Furthermore, the density of the MgO thin film was calculated from the refractive index by the Lorentz-Lorentz equation [35]:

$$\frac{n^2-1}{n^2+2}=\frac{N_A\rho\alpha}{3\varepsilon_0 M} \qquad (3\text{-}1)$$

Where n is the refractive index of the MgO film; N_A is Avogadro's number; M is the molecular mass; ε_0 is the permittivity of free space; ρ is the thin film density and α is the electrical polarizibility. Lorentz-Lorentz equation is one of the most powerful formulas to estimate thin film's density by measuring its refractive index and polarizibility first. By this approach, MgO bulk density can serve as a reference to modify the precise thin film density. The absorption coefficient in these experiments can also be measured by ellipsometer.

Chapter 4

Experimental Results and Discussion

4.1 Introduction

The performance of AC-PDP is critically dependent upon the properties of the MgO films in each cell. It is known that PDP is a promising candidate for large flat panel displays due to its unique characteristics with respect to display area, viewing angle, self-emitting image, power consumption, and high contrast ratio. Even though AC-PDP is probably the most promising candidate for large sized flat panel displays, there are some issues still remaining, which can not be ignored and affect the image quality of AC-PDP significantly.

In particular, MgO plays an important role as a protective layer in igniting and sustaining the plasma owing to its high secondary electron emission coefficient (γ), sputtering resistance and high transparency. However, the effect of density of the MgO film on PDP performance is not clear. To our knowledge, no previous report has appeared in the literature in which the relationship between the density of MgO films and AC-PDP properties has been investigated. Accordingly, it is believed that image sticking phenomenon is caused from the activation of MgO thin film and the deterioration of the phosphor layer [36] in AC-PDP. On the other hand, several driving methods to reduce the effect of image sticking phenomenon have already been proposed [37–38], but the investigation of the material part is still unclear.

It is believed that PDP performance is strongly influenced by the surface characteristics of MgO thin films because the film is exposed to the plasma. In this study, the deposition parameters are optimized and the relationship between the density of the MgO films and the properties of the AC-PDP is investigated. The

influence of MgO density and surface morphology on panel properties has been examined in accelerated aging tests.

4.2 MgO thin Film Density

The experiment is designed to characterize the effect of relationship between MgO thin film density and panel properties. Table 4.1 shows the density of MgO thin films for each of the experimental PDP modules. In this work, the density of the MgO thin films is calculated by substituting the thin film refractive index and ploarizibility into the Lorentz-Lorentz equation. As noted earlier, the refractive index was measured by ellipsometer. For measurements of the MgO film polarizibility, bulk MgO served as a reference. We assumed that MgO thin film and bulk MgO have same polarizibility. Therefore, the trend of MgO thin film density could be confirmed by this method.

Table 4.1 The MgO thin film density of each experimental PDP module formed with different oxygen flow rates. Panel No. 6 has the highest MgO thin film density 3.42 g/cm^3 while panel No.2 has the lowest MgO thin film density 3.22 g/cm^3.

	O_2 flow rate	Refractive index	MgO thin film density
No.1	40	1.644	3.29
No.2	***50***	***1.627***	***3.22***
No.3	40	1.632	3.24
No.4	40	1.645	3.29
No.5	40	1.640	3.27
No.6	***10***	***1.677***	***3.42***

Use Lorentz-Lorentz equation to estimate the MgO thin film density,

$$\frac{n^2-1}{n^2+2}=\frac{N_A\rho\alpha}{3\varepsilon_0 M} \qquad (3\text{-}1)$$

Avogadro's number N_A is 6.02×10^{23}; The electrical polarizibility α is 1.169×10^{-34} Å^3; The permittivity of free space ε_0 is 8.854×10^{-12} s^4 F/m; The molecular mass of MgO is 24, refractive index of each different oxygen flow rates formed MgO thin film is shown in the table; ρ is the thin film density.

As shown in Table 4.1, it indicates that panel No. 6 has the highest MgO thin film density 3.42 g/cm^3 while the lowest one goes to panel No. 2 and is only 3.22 g/cm^3. Panel No.6 has the lowest oxygen flow rate (10 sccm) during the evaporation, but forming into the thin film with highest density 3.42 g/cm^3; On the other hand, panel No. 2 has the lowest oxygen flow rate but forming into the thin film with lowest density 3.22 g/cm^3. The other panels' thin film density locates between 3.24 g/cm^3 to 3.29 g/cm^3. Under this circumstance, oxygen flow rate during the evaporation may play a key role affecting the formation of MgO thin film.

During the deposition process of MgO films, oxygen flow rate affects the stoichiometry of the film and, hence, the thin film density. A lower oxygen flow rate results in an increased MgO thin film density accompanied by a uniform but relatively rough surface. Higher MgO thin film density is often correlated with improved crystal structure, which yields to increased sputtering resistance and better luminance performance.

Since the MgO thin film is grown at different oxygen flow rate, the chamber environment may influence the stoichiometry of the Mg and the O molecules. Furthermore, the change of MgO stoichiometry during the formation also affects the thin film density and surface morphology of the MgO layer.

We believed that a relatively rough MgO surface can provide stronger wall charge for plasma ignition, which implies that the ignition and sustain voltages for the plasma are reduced owing to the increased surface area. Thus, a uniform but relatively rougher surface morphology provides a wider dynamic margin for the driving of a plasma display panel. As a result, higher MgO thin film density can be the reason that the panel provides a desirable performance. The relationship between refractive index and MgO thin film density is shown in Fig. 4.1. It shows that thin film density is proportional to the refractive index.

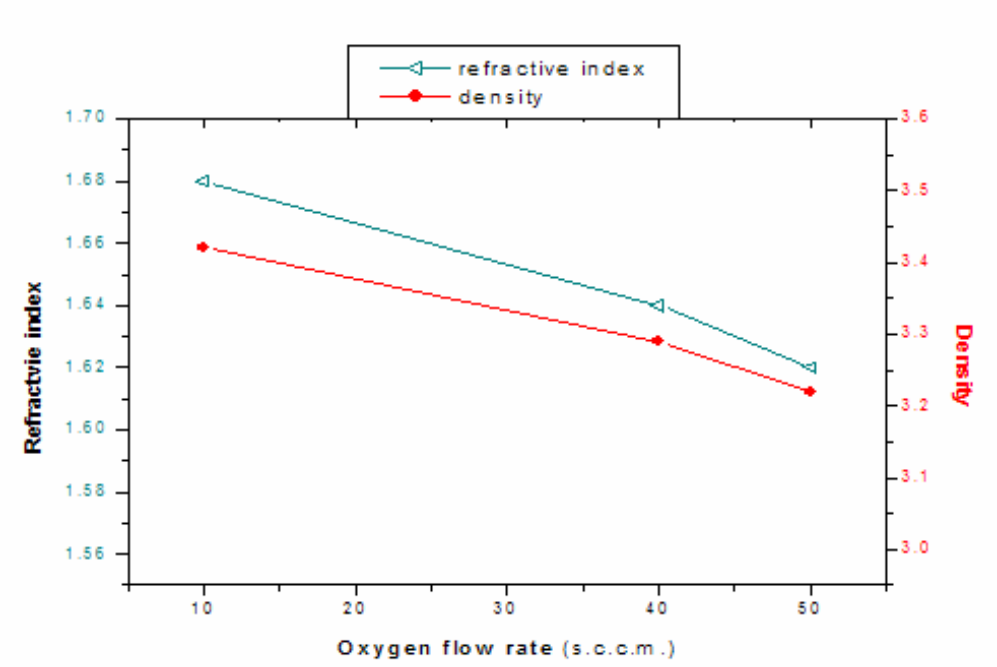

Fig. 4.1 The relationship between MgO thin film density and thin film refractive index for different oxygen flow rates formed MgO thin film. It shows that thin film density is proportional to the refractive index.

4.3 Dynamic Margin and Response Time

Figure 4.2 shows the variation of the dynamic margin as a function of time. For the driving concern, dynamic margin is defined as the area that specifies a normal driving voltage range for the experimental PDP modules. Generally, if the driving voltage or sustain voltage is outside the normal driving area, an overwriting or insufficient writing condition occurs, and often accompanied by the flickering effect.

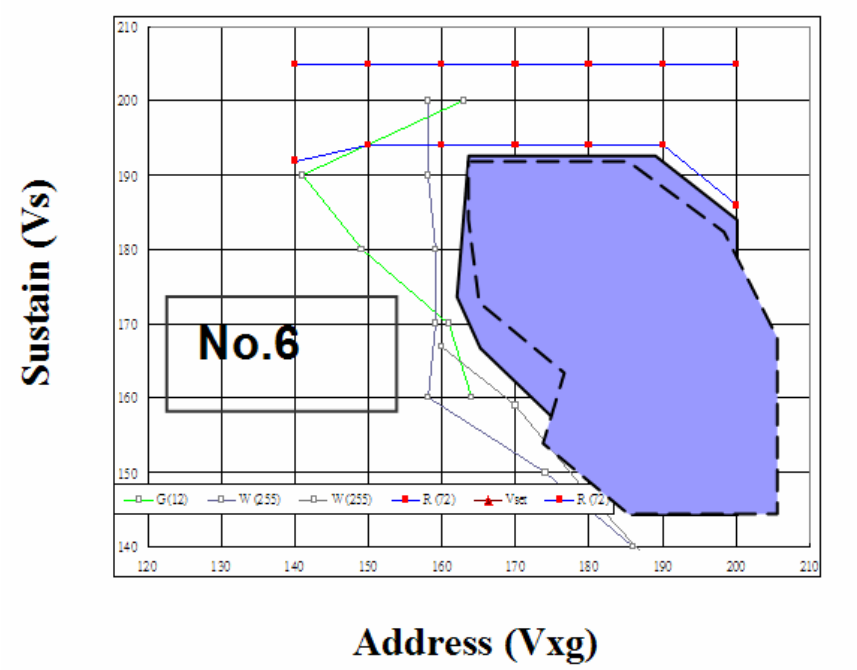

(a)

Fig. 4.2 (a) The dynamic margin of panel No.6. The solid line represents the dynamic margin before aging process while the dot line representing the dynamic margin after 100 hours aging.

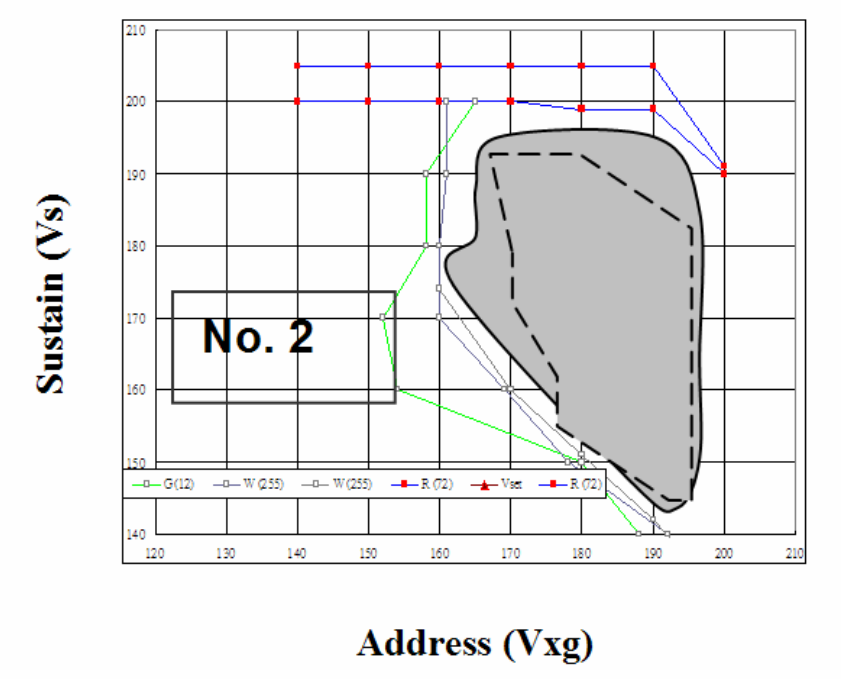

(b)

Fig. 4.2 (b) The dynamic margin of panel No.2. The solid line represents the dynamic margin before aging process while the dot line representing the dynamic margin after 100 hours aging.

Considering the dynamic margin observation, because green color is always relatively unstable compared to other colors, so the specific gray level selection in this experiment comprises with white (255), blue (255) and green (12). Green color is extremely unstable while the gray level is under 12. Therefore we choose green (12) to be the margin boundary. The horizontal axis represents the address voltage, V_{xg} and the vertical axis represents the sustain voltage, V_s, respectively. As shown in Fig. 4.2, the solid line illustrates the dynamic margin before aging process. After 100 hours of the aging process, the dynamic margin shifted to the dot line. During the life aging test period, panel discharge condition may have some difference. In this work, we found that panel No.6 and No. 2 present the biggest difference result on the dynamic margin.

In Fig. 4.2(a), the dynamic margin of panel No. 6 (10 sccm) maintained its original properties while that of panel No. 2 (50 sccm) decreased by about 20% as shown in Fig. 4.2 (b). Thus, there is a larger dynamic margin shift for panel No. 2 compared to panel No.6. We came upon that during the aging process, MgO thin film served as a protective layer formed with 10 sccm in panel No.6 may provide better protection against the plasma damage and ion bombardment. With superior protection, MgO thin film surface has less damage and lower sputtering rate. Degraded MgO surface would cause a unstable discharge condition, so the driving or sustain voltage may deviate and result in erratic dynamic margin. This may be the reason why panel No.6 maintained its dynamic margin but panel No.2 lost about 20% of the dynamic margin tolerance. As a result, the PDP module accompanied with MgO thin films grown at a lower oxygen flow rates holds stable condition in dynamic margin.

On the other hand, the discharge lag of each experimental PDP module did show significant difference before the aging process. Before 100 aging test, Panel No. 6 has the smallest discharge lag, which means the fastest response time around 480 ns, as shown in Fig. 4.3(a). Panel No. 2's and No.3's discharge lag are both around 568 ns as shown in Fig. 4.3(b). Other three panels' (No. 1, No. 4, and No. 5) discharge lag are 536 ns, 560ns, and 560 ns, respectively, as shown in Fig.4.3(c) and (d). But after 100 hours aging, discharge lag of panel No. 6 turned to around 550 ns while that of panel No. 2 turned to about 1000 ns, which is almost two times longer than No.6's. Once again, panel No. 6 achieved the best performance while panel No.2 went to the worst one.

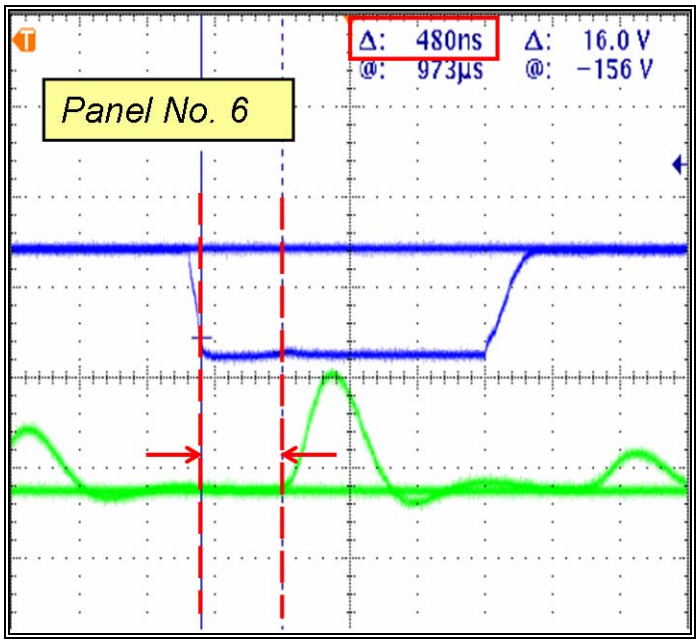
Δ: 480ns
@: 973µs
Δ: 16.0 V
@: −156 V
Panel No. 6

(a)

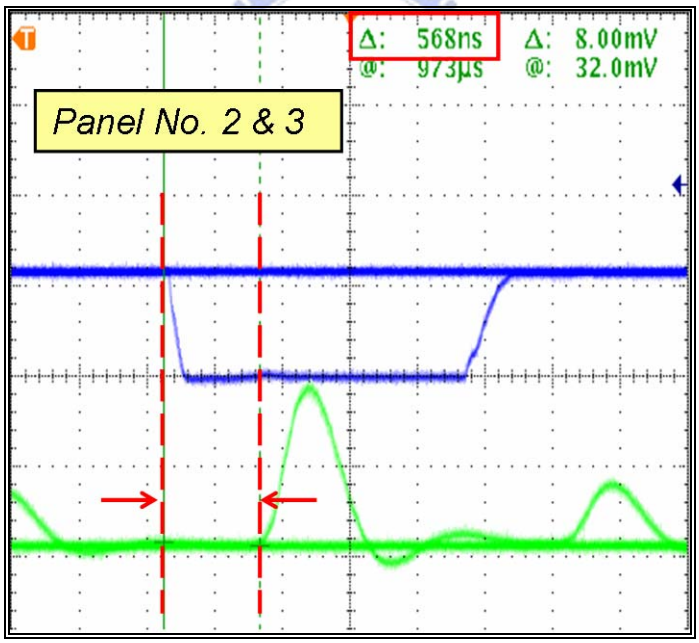
Δ: 568ns
@: 973µs
Δ: 8.00mV
@: 32.0mV
Panel No. 2 & 3

(b)

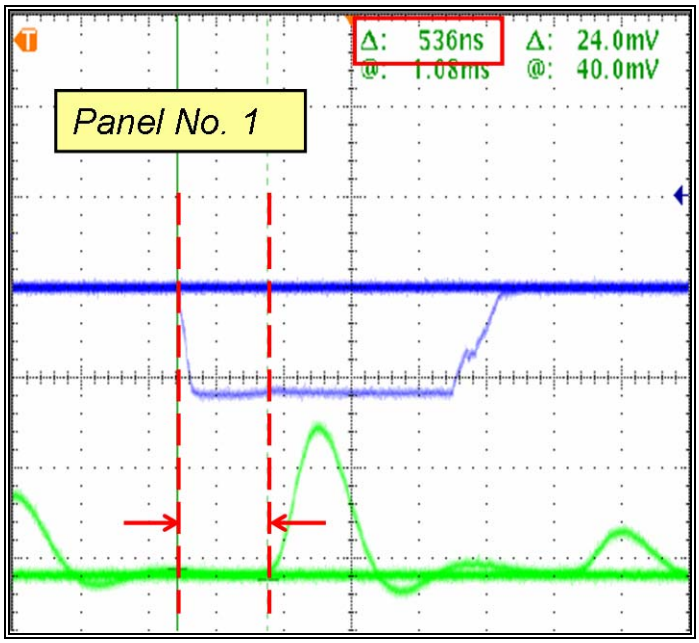

(c)

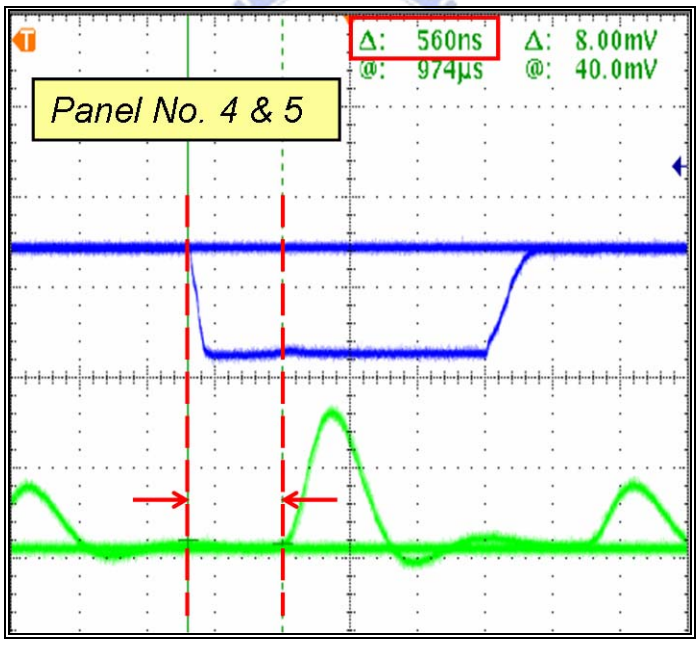

(d)

Fig. 4.3 The discharge lag of each experimental PDP module used in this study. It displays the response time of (a) No. 6; (b) No. 2 and No. 3; (c) No. 1; (d) No. 4 and No. 5, respectively.

4.4 Luminance Degradation

In this paragraph, the luminance degradation of each experimental PDP module would be investigated. Luminance of red, green, and blue color was recorded as a function of time from zero hour to 1500 hours with the aging process. The continuous lighting up condition would affect the panel performance. We believe that the consecutive plasma and ion bombardment would sputter the MgO surface and cause damage to the panel properties. Luminance degradation becomes serious under this circumstance.

Figure 4.4 illustrates the luminance degradation of experimental PDP modules as a function of time. We measured the luminance of a red, green and blue color pattern in the center of each panel at t = 0, 100, 500, 1000 and 1500 hours. As expected, the luminance of each experimental panel decreased as a function of operating time.

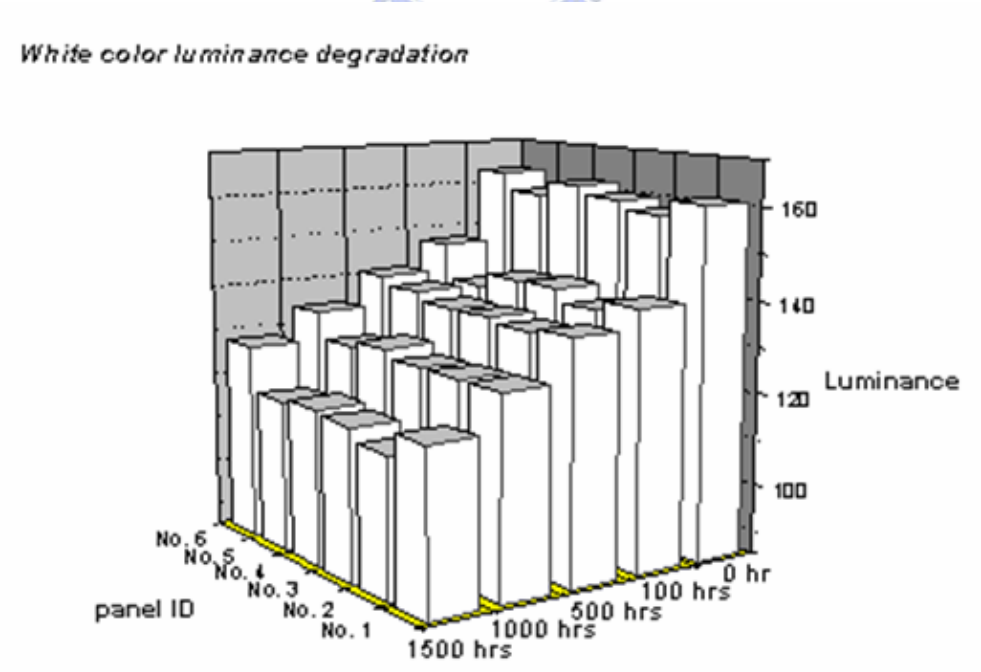

Fig. 4.4(a) The white color luminance degradation of each experimental PDP module as a function of operating time from zero to 1500 hours.

4.4.1 White Color Luminance Degradation

It shows the luminance variation of white color in Fig. 4.4(a). At the beginning of the experiment, white color luminance of panel No. 6 was 163 cd/m^2 while panel No. 2 was only 158 cd/m^2. Accordingly, even before the aging process, panel No. 6 has the highest luminance performance compared to other panels. Panel No. 1 has second best performance on luminance 161 cd/m^2.

After a 1500 hours life aging test, the white color luminance of panel No. 6 went down to 128 cd/m^2 while No. 2 went down to 113 cd/m^2. The luminance decreased around 21.5 % after 1500 hours continuous aging while that of panel No. 2 decreased about 28.6 %. A similar phenomenon was observed for the other color patterns. Panel No. 6, incorporating MgO thin films deposited with the lowest oxygen flow rate, yielded the highest luminance accompanied by the lowest degradation.

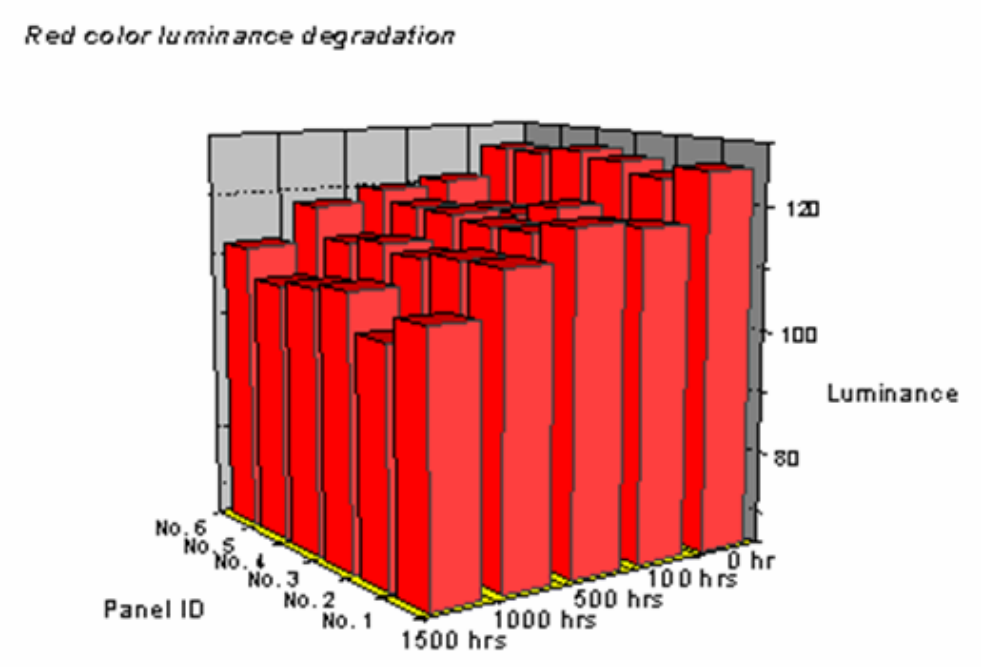

Fig. 4.4(b) The red color luminance degradation of each experimental PDP module as a function of operating time from zero to 1500 hours.

4.4.2 Red Color Luminance Degradation

As shown in Fig. 4.4(b), red luminance shows relatively smaller degradation than white color ones. At zero hour, red color luminance of panel No. 6 was 125 cd/m^2 while panel No. 2 was 122 cd/m^2. Thus, even before the aging process, panel No. 6 has the highest luminance performance compared to other panels. Panel No. 1 also has pretty good performance on luminance reaching to 125 cd/m^2 which equals to that of panel No.6. After a 1500 hours life aging test, the red color luminance of panel No. 6 went down to 111 cd/m^2 while No. 2 went down to 101 cd/m^2. The luminance decreased around 11.2 % after 1500 hours continuous aging while that of panel No. 2 decreased about 17.2 %.

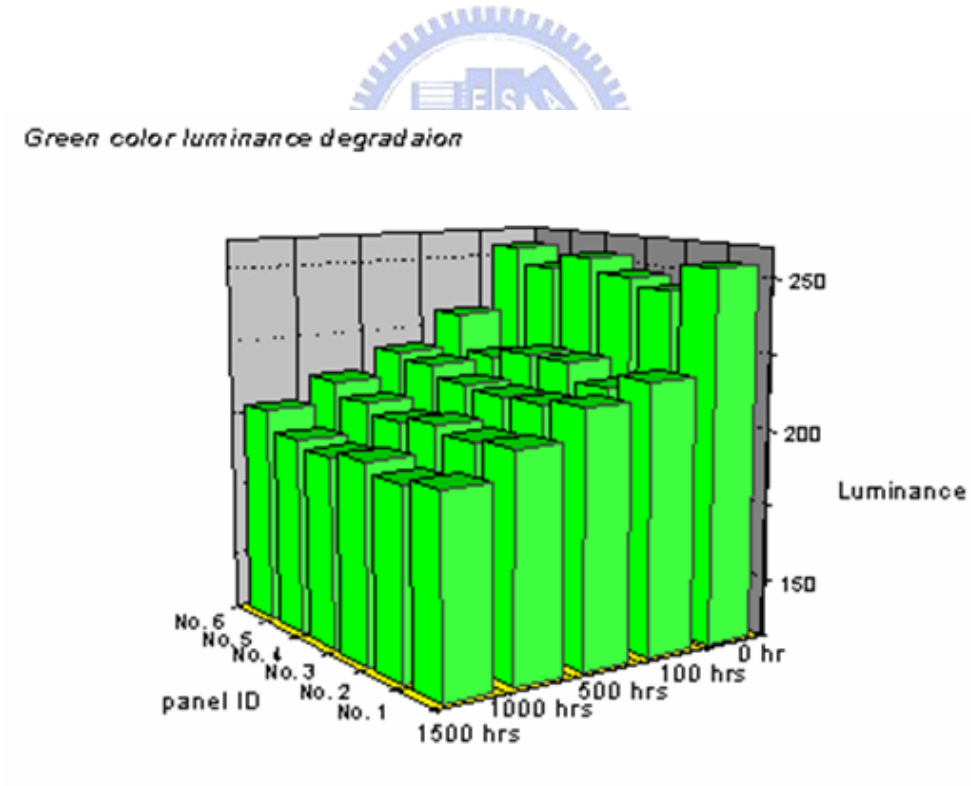

Fig. 4.4(c) The green color luminance degradation of each experimental PDP module as a function of operating time from zero to 1500 hours.

4.4.3 Green Color Luminance Degradation

As shown in Fig. 4.4(c), green luminance degradation shows similar variation with white color ones. At zero hour, green color luminance of panel No. 6 was 256 cd/m^2 while panel No. 2 was 243 cd/m^2. Just like noticed above, before the life aging process, panel No. 6 has the highest luminance performance compared to other panels. Panel No. 1 also has a quite match performance with panel No.6 reaching to 255 cd/m^2. After a 1500 hours aging process, the green color luminance of panel No. 6 dropped down to 202 cd/m^2 while No. 2 went to around 182 cd/m^2. The luminance decreased about 21.1 % after 1500 hours continuous aging while that of panel No. 2 decreased to a degree about 25.1 %.

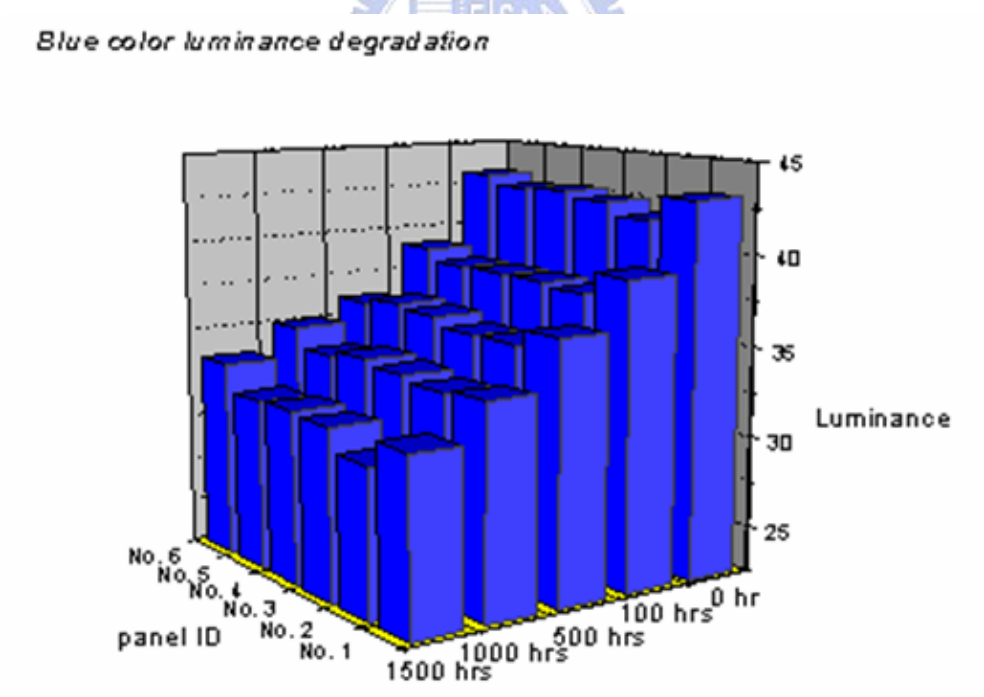

Fig. 4.4(d) The blue color luminance degradation of each experimental PDP module as a function of operating time from zero to 1500 hours.

4.4.4 Blue Color Luminance Degradation

As shown in Fig. 4.4(d), blue luminance is quite dark compared to other colors. At the beginning, blue color luminance of panel No. 6 was 43 cd/m^2 while panel No. 2 was 40.5 cd/m^2. Therefore, before the aging process, panel No. 6 has the highest luminance performance compared to other panels. Panel No. 1 at this point has the same performance going to 43 cd/m^2. After a 1500 hours aging process, the blue color luminance of panel No. 6 dropped down to 33 cd/m^2 while No. 2 reduced to around 28.5 cd/m^2. The luminance decreased about 23.2 % after 1500 hours continuous aging process while that of panel No. 2 decreased to a degree about 29.6 % which is the worst condition among all colors.

4.5 Color Temperature and Color Coordinates

Figure 4.5 illustrates the temporal variation of the color temperature of the experimental PDP modules. At t = 0, panel No. 6 had the highest white color temperature (6050), while panel No. 2 had the lowest white color temperature (5950). However, after the aging process, panel No. 6 shows the largest color temperature variation.

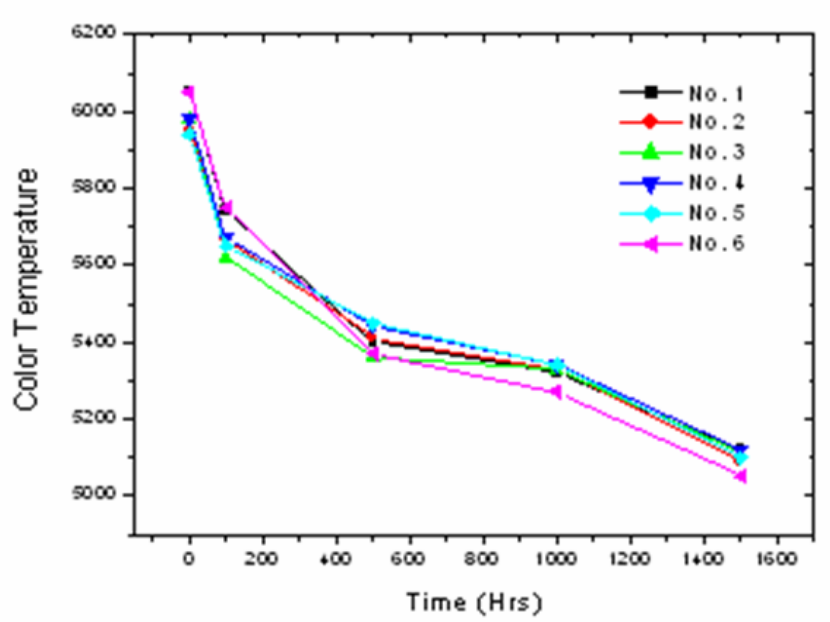

Fig. 4.5 The color temperature variation of each experimental PDP module as a function of operating time from zero to 1500 hours.

4.6 Image Sticking Phenomenon

For the image sticking observation, the test pattern adopted for the use of image sticking observation is generated by the pattern generator Axtro-828. Color analyzer CA-100 is used to detect the luminance, color temperature, and color coordinate of the selected patterns. In order to inspect the recover ability from the image sticking of different panels, panel performance such as luminance degradation and color coordinate variation of bright and dark backgrounds were investigated and recorded as a function of time.

Figure 4.6(a) shows the experimental PDP module and (b) investigation system of this experiment. For the image sticking phenomenon observation, we display a full white 255 gray level square pattern in the center of the panel. The pattern is displayed continuously for 30 minutes in order to warm up the panel and normalize the initial condition. Luminance degradation is recorded as a function of operation time in order to make sure the discharge condition is stable for the observation.

Fig. 4.6(a) The experimental PDP module using for the image sticking phenomenon observation. A full white 255 gray level square pattern is displayed in the center of the panel.

Fig. 4.6(a) The optical measurement system using for the image sticking observation. CA-100 is used to record luminance, color coordinates, and color temperature of the selected pattern.

As shown in Fig. 4.7(a) and (b), it illustrates the typical white image sticking and dark image sticking phenomenon. Generally, white image sticking phenomenon appears after the very display pattern being written repeatedly and then turning into a full white image. Take Fig. 4.6(a) and 4.7(a) as an example. If the white square pattern displayed in the center of the panel continuously for several minutes, and then change the pattern to a full white 255 gray level rapidly, the ghost image would appear replacing the previous white square with a darker one as shown in Fig. 4.7(a). Vice versa, the dark image sticking phenomenon happens while the pattern change to a full dark background. The ghost image emerges to replace the previous white square pattern with a relatively brighter image but a full dark pattern.

Furthermore, it is believed that image sticking phenomenon is caused from the activation of MgO thin film and the deterioration of the phosphor layer. More precisely, white image sticking is considered to be related with the activation of MgO thin film. After the continuous gas discharge and ion bombardment to the MgO

surface, the center square results into a highly activated MgO which is temporary different from the other part. Hence, the discharge and breakdown condition is also different from other area. This could be the reason that ghost image shows up in the center of the panel.

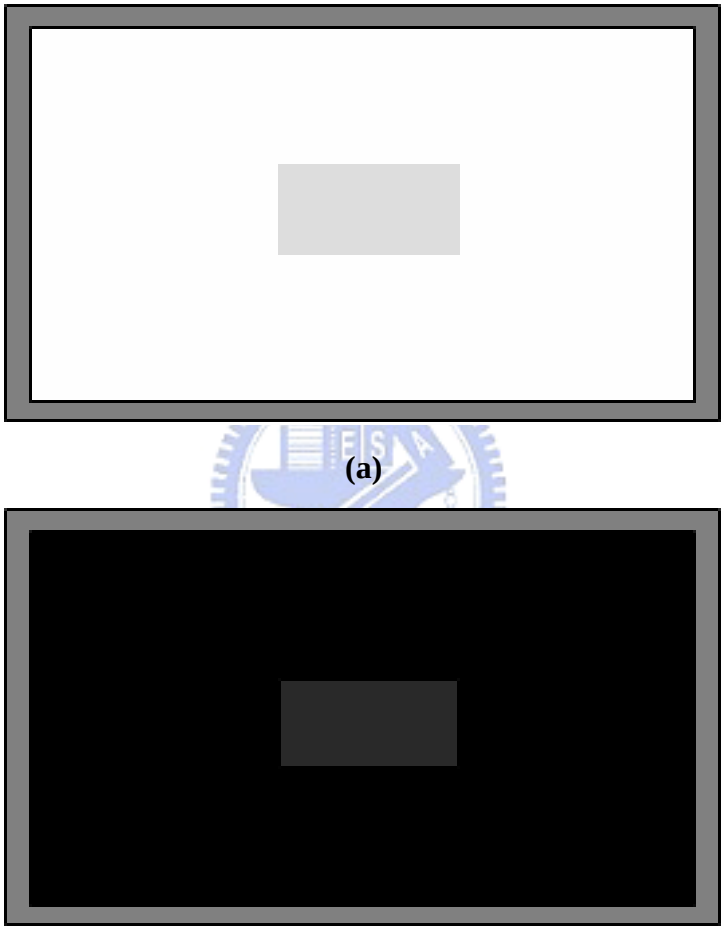

(a)

(b)

Fig. 4.7(a) The typical white image sticking and (b) dark image sticking phenomenon. A relatively dark ghost image would appear.

On the other hand, dark image sticking is considered to be related to the deterioration of phosphor material. Since the panel is going to be full dark to make dark image sticking, it denotes that there will be no gas discharge or plasma occurs at the full dark stage. Under this circumstance, MgO served as a protective layer has no significant effect on the dark image sticking phenomenon. It is believed that before the panel turning into a full dark background, the white square pattern causes the temperature rising during the sustain period. This temperature variation may deteriorate and stimulate the phosphor layer. Thus, even the panel was designated to be full dark, but this deteriorated or stimulated phosphor would provide relatively bright image in the center than other area of the panel.

Additionally, several driving methods to reduce the effect of image sticking phenomenon have already been proposed, but the investigation of the material part is still unclear. Even though there was some research for the image sticking issue in AC-PDP, it hasn't provided any results to verify the relationship between the image sticking and the panel properties yet. Therefore, the focus has been put on to the influence of MgO thin film on the image sticking phenomenon in AC-PDP.

4.6.1 Pre-Work

In order to observe the trend of luminance variation and investigate image sticking phenomenon in AC-PDP, both the center and outside luminance degradation is recorded. Since oxygen flow rate seems to be a key factor for MgO formation, we focus on the comparison of panel No. 6 and No. 2 in the image sticking observation. Figure 4.8 illustrates the luminance degradation in the center square and outside area of both panels as a function of display time. In this progress, we didn't apply any special pattern to the panels in order to normalize the initial condition. The result shows that luminance in different parts of the panel remains almost the same, which

means the discharge condition is approximate stable in each cell during the sustaining period.

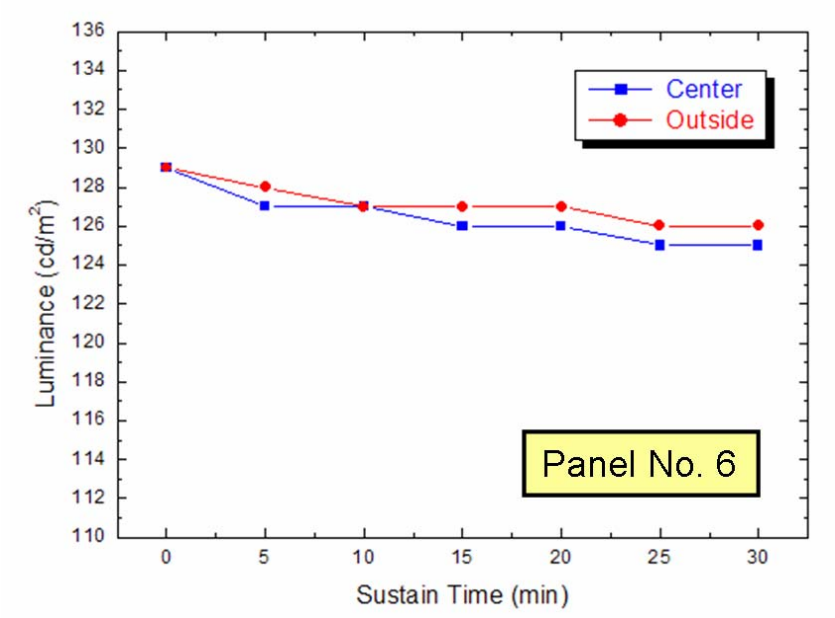

(a)

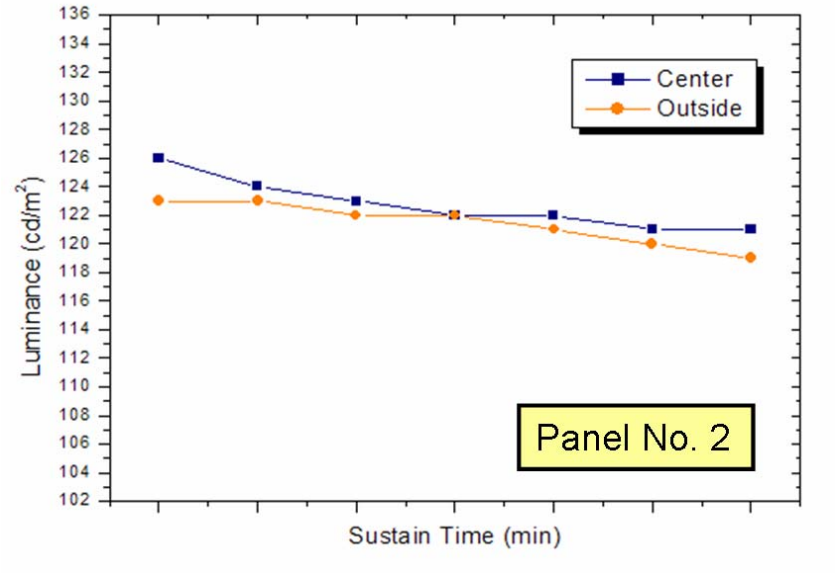

(b)

Fig. 4.8 Luminance degradation of (a) panel No. 6 (10 sccm) and (b) panel No. 2 (50 sccm) before the image sticking phenomenon observation.

4.6.2 White Image Sticking

After a white color square pattern with 255 gray level is displayed repeatedly at the center of the panel, the image pattern is then changed into a full white background. Therefore, the original white square pattern in the center becomes relatively darker, which is the white color image sticking phenomenon appearing on the panel.

Figure 4.9(a) shows the image sticking phenomenon of panel No. 6 in a white background sustained from zero to 30 minutes. Luminance of the center square in the panel decreases rapidly with the pattern turning into a full white color background after being sustained continuously for 5 minutes. However, the luminance difference between center square and periphery will become stable after the sustaining time prolongs more than 10 minutes. With a PDP module being sustained more than 5 minutes, there exists a luminance disparity around 11.8% between the image sticking cells and the normal ones. For the panel No. 2, whose MgO thin films was formed by 50 sccm O_2 flow rate, white color image sticking phenomenon is shown in Fig 4.9(b). The luminance difference proves to be relatively stable when the sustaining time extends more than 10 minutes, but disparity comes to the end around 13.6%, which is severe than panel No. 6. As a result, panel No. 6 with MgO thin film formed with a lower O_2 flow rate provides better performance against white image sticking problem.

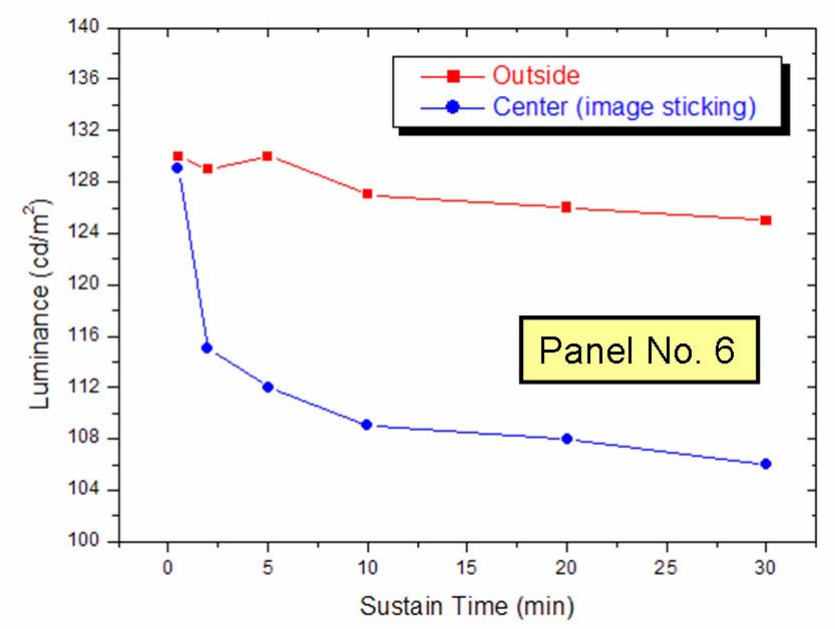

(a)

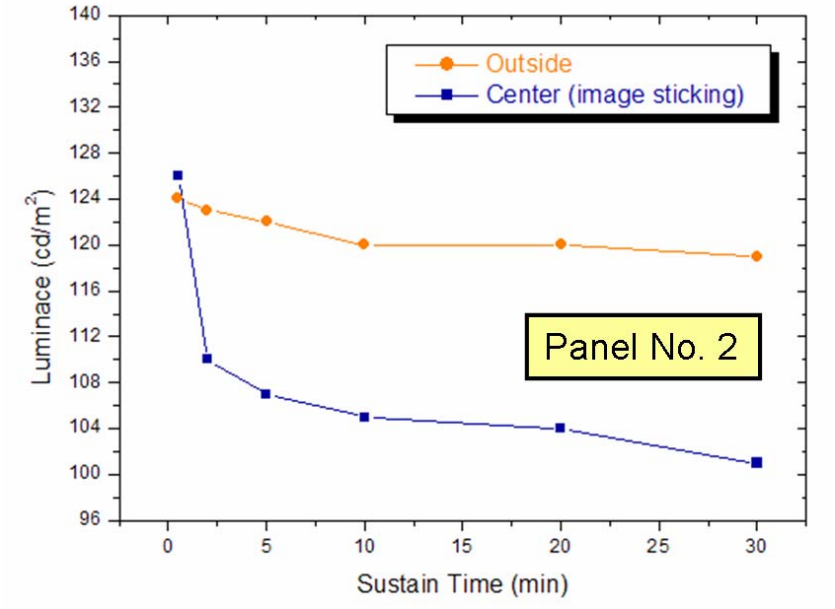

(b)

Fig. 4.9 White luminance degradation of image sticking cells and normal operated ones in (a) panel No. 6 (10 sccm) and (b) panel No. 2 (50 sccm) after 30 minutes sustain period.

4.6.3 Dark Image Sticking

It is reported that white color image sticking always results from the activation of MgO layer while black (dark) image sticking comes from the deterioration of phosphor layer. Dark color (black) image sticking phenomenon appears when the panel turns into a totally dark background after the selected pattern was continuously displayed for a period of time. The original white center square will still have a relatively bright image even though the pattern is changed to make a full dark background. Generally, it is believed that the rise of temperature due to the continuous sustain pulse may deteriorate the phosphor layer. Figure 4.10(a) and (b) show the luminance of dark image cells and normal operated ones of panel No.6 and No.2, respectively. The image sticking cells provide relatively higher luminance than that of the non-image sticking cells, which is exactly contrary to the white image sticking phenomenon. According to our investigation, when it comes to dark image sticking phenomenon, panel No. 1 has better performance than panel No. 2. After the image sticking phenomenon stabilized, which means that sustain time extends more than 10 minutes, luminance difference between the ghost image and the normal image of panel No. 1 and No. 2 is around 14.2% and 17.3%, respectively.

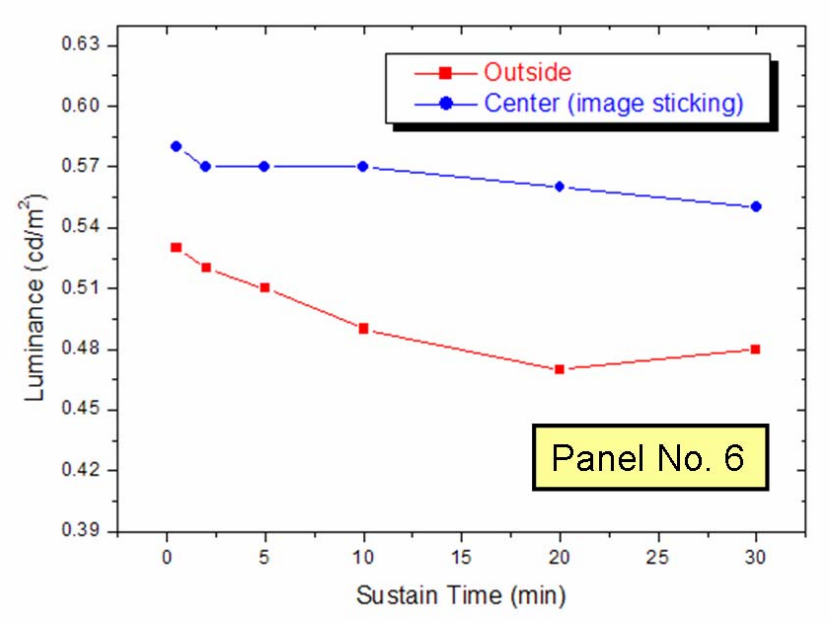

(a)

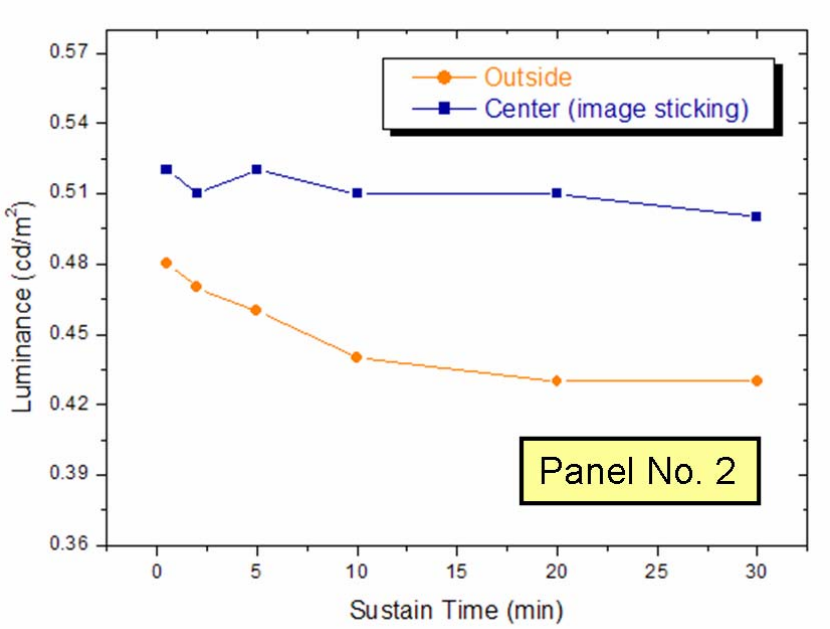

(b)

Fig. 4.10 Dark luminance degradation of image sticking cells and normal operated ones in (a) panel No. 6 (10 sccm) and (b) panel No. 2 (50 sccm) after 30 minutes sustain period.

4.6.4 Color Temperature

Figure 4.11(a) and (b) illustrate the color temperature variation of white color image sticking in panel No. 6 and No.2 as a function of display time. The image sticking cells provide relatively lower color temperature than the normal discharge cells do. In the beginning, color temperature drops critically when the sustain time is up to 5 minutes. After that, it becomes more stable when the sustaining time is longer than 10 minutes. In this situation, we conclude that color temperature variation may have more relationship with phosphor than MgO protective layer.

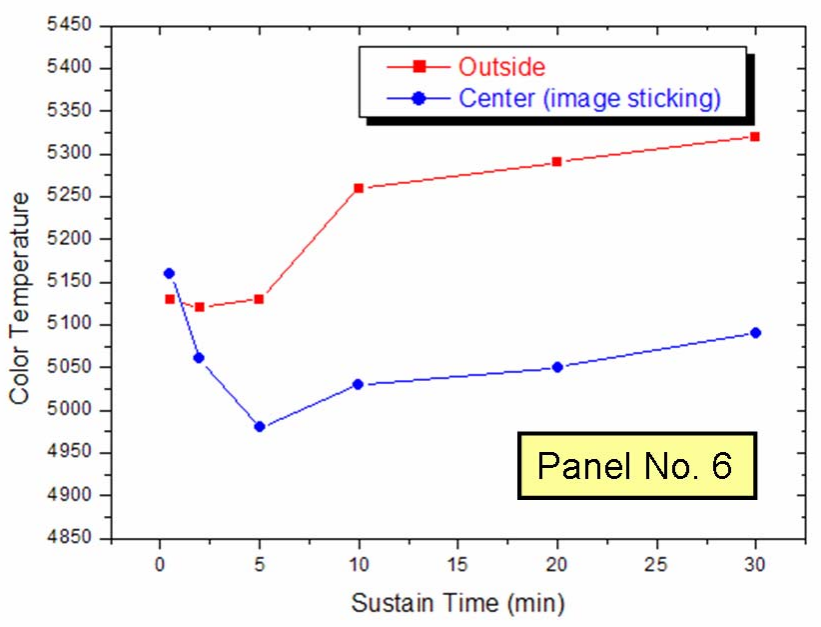

(a)

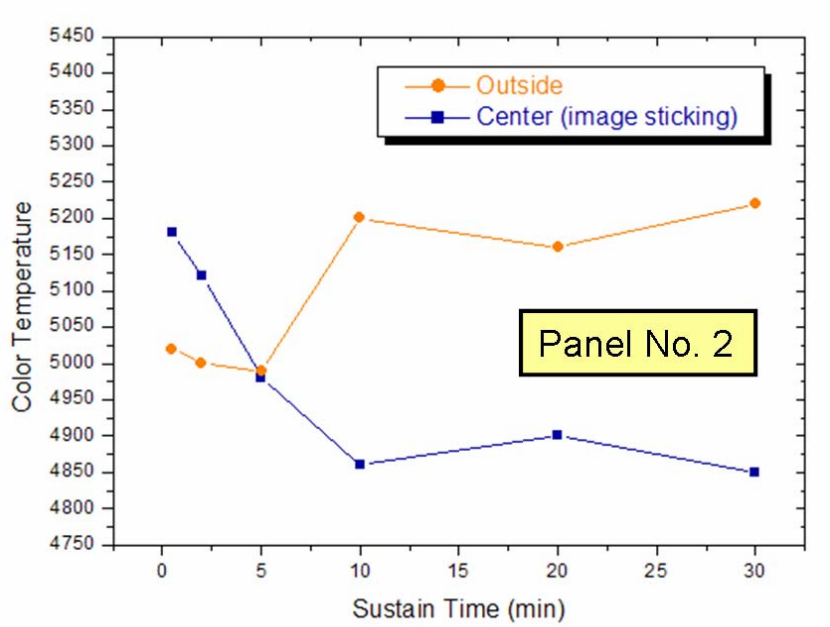

(b)

Fig. 4.11 Color temperature variation of image sticking cells and normal operated ones in (a) panel No. 6 (10 sccm) and (b) panel No. 2 (50 sccm) after 30 minutes sustain period.

4.6.5 Recovery Ability

One thing to evaluate image sticking phenomenon is to estimate that how fast could the ghost image (image sticking) disappear and then recover to a normal condition as expected. In Fig. 4.12(a) and (b), we demonstrate the recovery ability by calculating the luminance disparity percentage of the image sticking cells to the normal discharge ones. It reveals that a PDP module with MgO thin film grown at relatively lower O_2 flow rate (10sccm) exhibits superior recovery ability compared to that of whose MgO thin film is grown at higher O_2 flow rate (50 sccm).

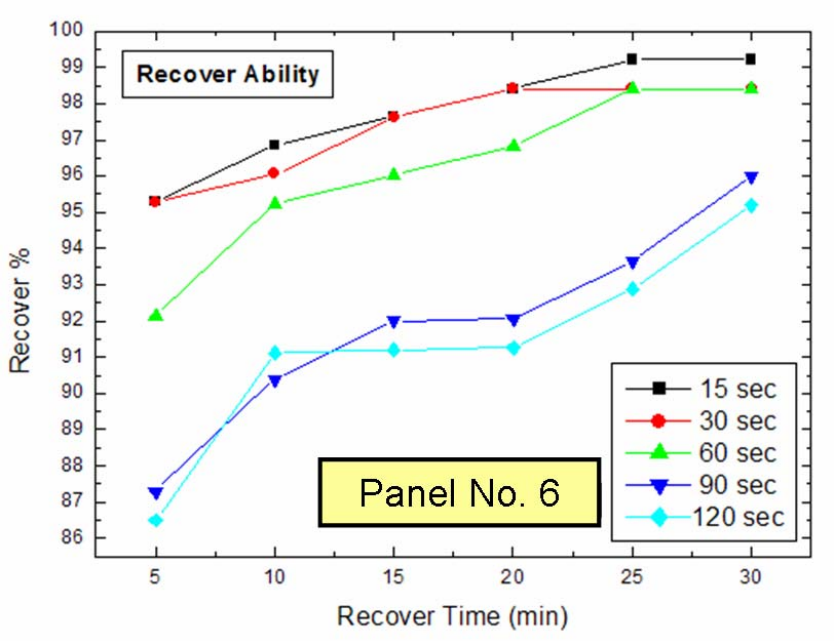

Fig. 4.12(a) The recovery ability of panel No. 6 for the image sticking observation. It shows the recover time for panel No.6 with different sustain time (15sec to 2 min).

In Fig. 4.12(a), for the 10 sccm formed MgO thin film panel, image sticking cells recuperate more than 90% in 11 minutes when the pattern is sustained and displayed less than 2 minutes. For the 50 sccm case, it takes about 15 minutes for the ghost image to disappear and approach close to 90% as shown in Fig. 4.12(b). After the panel turns into a full white background and then left for 30 minutes, the recovery situation for panel No.6 regains more than 95% if the previous pattern is displayed less than 2 minutes. For panel No. 2, it takes more than 34 minutes for the ghost image recover to 95% if the previous pattern is displayed less than 2 minutes.

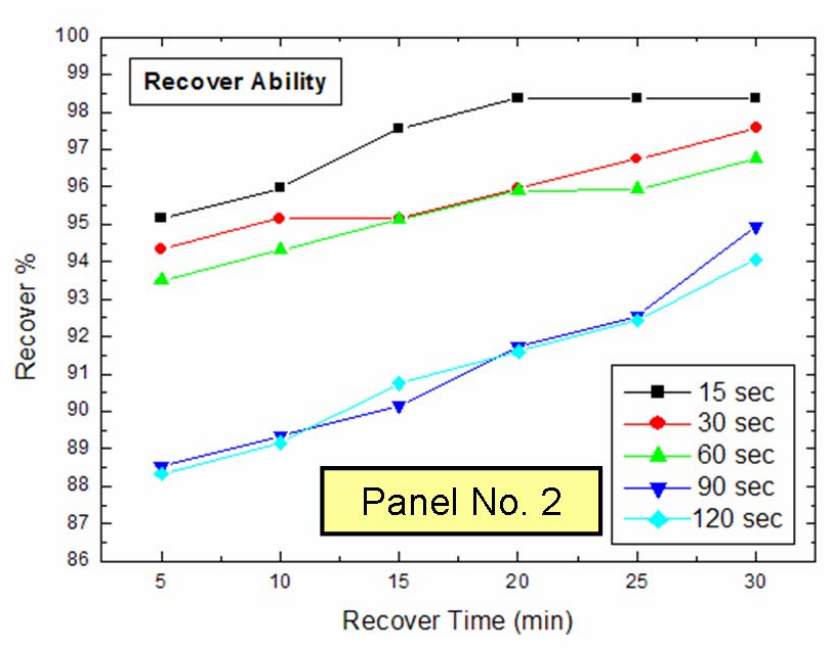

Fig. 4.12(b) The recovery ability of panel No. 2 for the image sticking observation. It shows the recover time for panel No.6 with different sustain time (15sec to 2 min).

4.7 Analysis of Surface Morphology – AFM

Figure 4.13 is the AFM image of MgO thin films incorporated into the experimental PDP modules. Figure 4.13(a) shows the surface morphology of the MgO thin film from panel No. 6. It reveals that lower oxygen flow rate would result in a uniform but relatively rough MgO surface. The root mean square (RMS) roughness of MgO thin film with 10 sccm O_2 flow rate is 7.63 nm.

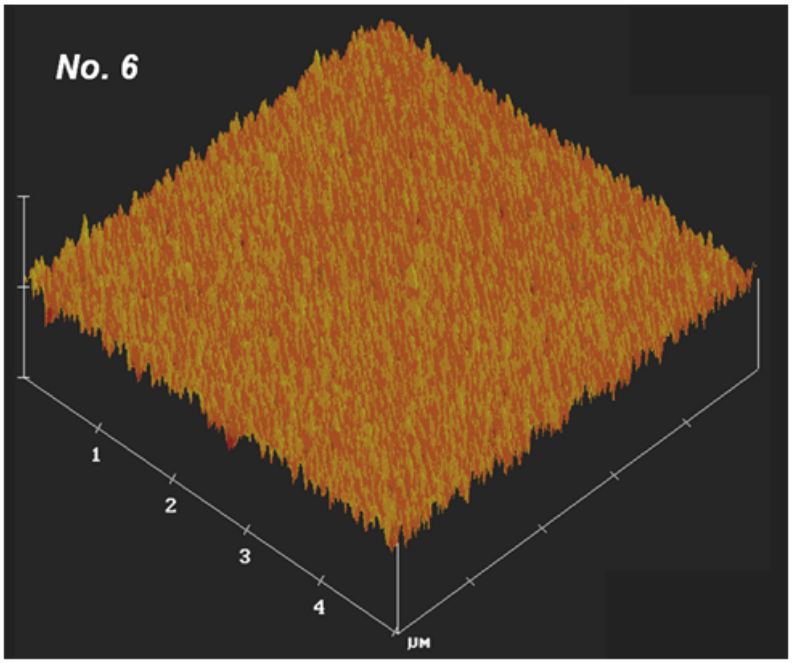

Fig. 4.13(a) The AFM image of MgO thin film surface in panel No. 6. The RMS roughness is 7.63 nm.

Figure 4.13 (b) shows the MgO surface morphology of the MgO thin films from the panel No.2. It manifests that lower oxygen flow rate would produce a relatively rough MgO thin film surface. The root mean square (RMS) roughness of 50 sccm growth MgO thin film is 6.29 nm.

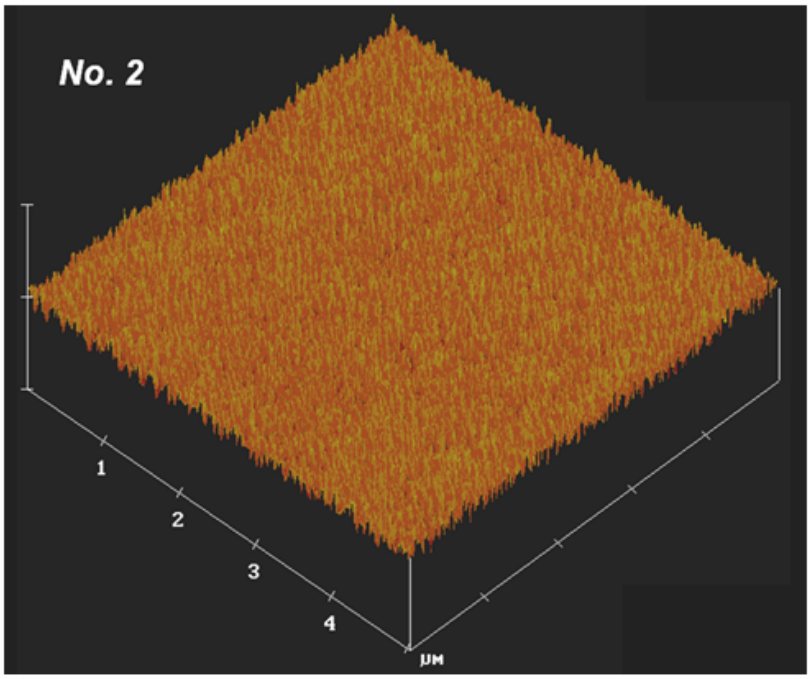

Fig. 4.13(b) The AFM image of MgO thin film surface in panel No. 2. The RMS roughness is 6.29 nm.

According to the boundary conditions for the electric fields, the normal component of the electric flux density (dielectric displacement D) field is discontinuous across an interface where a surface charge exists and the degree of the continuity is proportional to the surface charge density [41]. Since surface charge accumulates in regions with sharp surface relief, it is believed that a uniform but relatively rougher MgO surface may help to gather wall charge and favor to provide stronger plasma ignition, which implies that the ignition and sustain voltages for the plasma are reduced owing to the increased surface area. Thus, relatively rough surface morphology provides a wide dynamic margin for the driving condition of a plasma display panel. Stronger crystallinity of MgO thin film (which will be discussed in 4.8) can contribute to emit more secondary electrons by the ion bombardments. Accordingly, the plasma can be ignited and sustained easily.

4.8 Investigation of Crystal Structure –XRD

Figure 4.14 shows the X-ray diffraction (XRD) spectrum of MgO thin films in the experimental PDP modules. The (1 1 1) peak at the left-hand side represents the preferred orientation of MgO thin films. The peaks on the right-hand side and at center arise from the metal holder. Figure 4.14(a) shows that the MgO thin films of panel No. 6 exhibit a strong (1 1 1) peak (2θ= 37.8°). Figure 4.14(b) shows the XRD spectrum of MgO thin film from panel No. 2. This spectrum confirms the inference that a lower oxygen flow rate provides a higher degree of crystallinity and increased thin film density. We believe that the predominant (1 1 1) orientation and excellent crystal structure of panel No. 6 results from the dense MgO thin film with the lower oxygen flow rate.

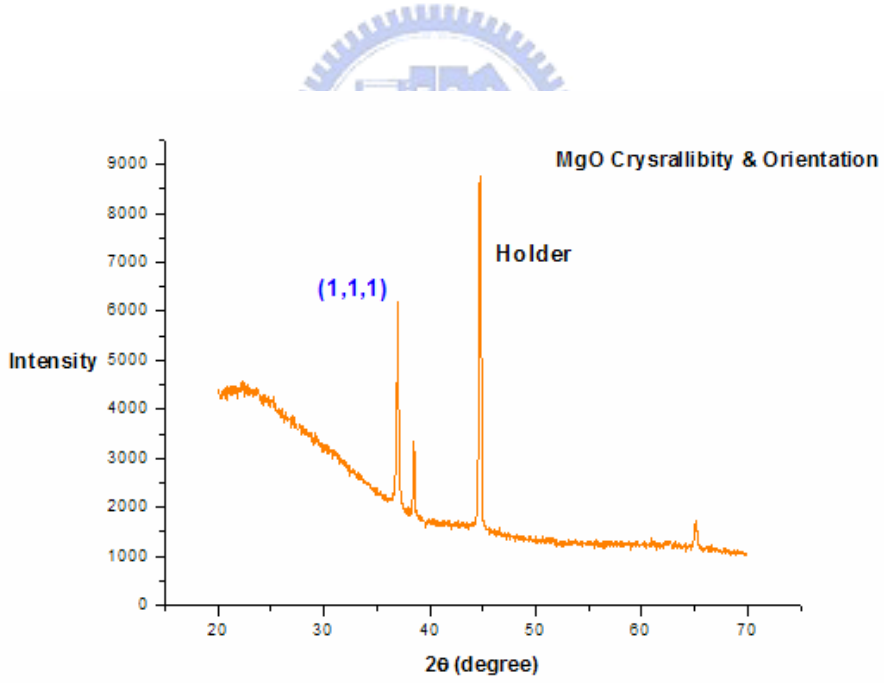

Fig. 4.14(a) The XRD spectrum analysis of MgO thin film formed at 10 sccm O_2 flow rate in panel No. 6.

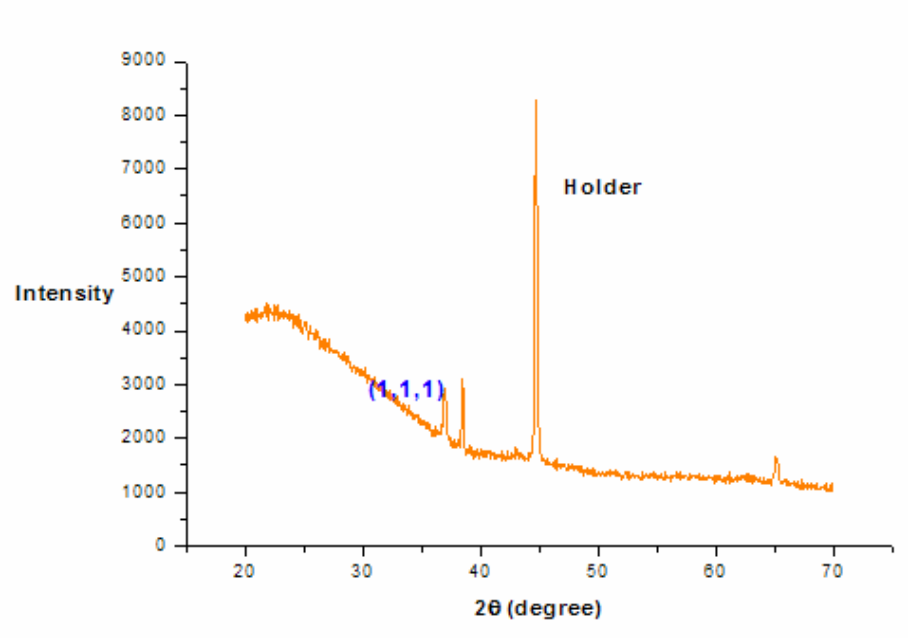

Fig. 4.14(b) The XRD spectrum analysis of MgO thin film formed at 50 sccm O_2 flow rate in panel No. 2.

4.9 Summary

The MgO thin film density of panel No.6 (10 sccm) and panel No.2 (50 sccm) are 3.42 g/cm^3 and 3.22 g/cm^3, respectively. By atomic force microscopy (AFM) and X-Ray diffraction (XRD), it reveals that MgO thin film grown at lower oxygen flow rate (10 sccm) possess a uniform but relatively rougher surface and a much stronger crystallinity. This uniform but relatively rougher surface is contributive in collecting the charges in the sharp area on MgO surface. Accordingly, the plasma can be ignited and sustained easily. Stronger crystallinity of MgO thin film can be a good shield to protect the dielectric layer from the ion bombardment. As a result, higher MgO thin film density can be the reason that the panel provides a desirable performance. In this study, we conclude that a PDP with MgO thin flms grown at low oxygen flow rate (10 sccm) has better performance including luminance, dynamic margin, response time, color temperature, smaller visual difference between image sticking cells and normal

operated ones, and superior recovery ability against image sticking. We presume that because of the high density and strong crystallinity, it results in a highly activated MgO thin film during the plasma ignition in the cell. It helps the MgO thin film surface of both image sticking cells and normal ones to gather charges easily and back to balance. Hence, after the panel turns into a full white or full dark background from the previous pattern, it shows relatively slight image sticking because of this “excellent” MgO thin film.

Chapter 5

Conclusion

5.1 Conclusion

As population of computer and internet communication, electronic products capable of light weight, thin volume and low power consumption are highly valued and demanded. As a result, industry of FPD is now growing up rapidly due to the demand of consumer electronic product market. Among those designs and products, big sized TV with thin volume and lower power consumption is now recognizes as the rising star. Until now, the market for direct-view, flat panel televisions was segmented fairly clearly, with LCD sets available only in screen sizes smaller than 50 inches, and PDP products available in larger screen sizes ranging from 37 to 102 inches. Moreover, it is believed that PDP is the promising candidate for the large sized TV and home theatre applications. Excellent image quality and necessary big size (more than 100 inches) give PDP the ability to fulfill the dream of building up home theatre in each family. With the innovation and newly developed technology, PDP can guarantee more than 60000 hours life to half luminance. Unlike LCD using back light source, PDP is a self-emissive display, which can provide wide viewing angle, makes it have a CRT like high image quality.

The large area FPD is demanded for a HDTV and a digital TV which displays a real and life-size image in addition to the traditional TV image because of the development of the both computer and network technologies. Plasma displays are now having an unprecedented degree of success as large-screen televisions (TVs). World sales of plasma display modules reached $6 billion in 2005. Sales are projected to be $8.9 billion by 2007. In the start of 2005, there shows the appearance of a high

quality 102-inch diagonal 1920 x 1080 pixel high definition plasma TV prototype. The U.S. based Consumer Electronics Association's October 2004 holiday forecast survey found that plasma TV was the most desired gift for the holiday season.

In this work, the relationship between MgO thin film properties and panel performance are investigated by demonstrating 46-inch WVGA type plasma display panel. During MgO formation, the combination of MgO and O molecular will be affected significantly by the evaporation condition. Electron beam evaporation is used to deposit MgO thin film as a protective layer on dielectric layer in the experimental PDP modules. Oxygen flow rate is characterized the most important factor in this study.

As a result, it is found that with lower oxygen flow rate (10 sccm) formed MgO thin film, better panel performance can be realized due to several reasons. Firstly, higher MgO thin film density can be achieved by importing lower oxygen flow rate during the evaporation. Second, excellent crystal structure and strong crstallinity can be accomplished to provide good sputtering resistance against plasma and ion bombardment. Third, a uniform but relatively rough surface structure is proved to help generate more wall charge and reduce the driving voltage. Panel performance including luminance, response time, dynamic margin, color temperature, and image sticking are investigated to prove the theory. Therefore, it is believed that lower oxygen flow rate formed MgO thin film can achieve better panel performance by its superior physical and chemical properties.

5.2 Future Work

Since image sticking phenomenon is now the hottest issue to achieve a desirable PDP, more work will be added to realize the relationship between MgO thin film and phosphor layer and image sticking. However, the improvement of better MgO thin film is also one of the most interesting topics to do. Through different fabrication process or different addition to MgO thin is believed to be capable to change the game too. Therefore, several methods will be proposed to investigate more detail about the MgO thin film in AC-PDPs.

Reference

[1] Larry Weber, “The promise of Plasma Displays for HDTV”, SID ‘00 Digest, pp. 402-405 (2001).

[2] The U.S. Consumer Electronics Association (2004).

[3] Betsui Keiichi, Namiki Fumihiro, Kanazawa Yoshikazu, Inoue Hiroshi, “High-resolution plasma display panel (PDP)”, Fujitsu Scientific and Technical Journal, Vol. 35, No. 2, pp. 229-239 (1999).

[4] www.howstuffworks.com (2002)

[5] C. H. Park, Y. K. Kim, B. E. Park, W. G. Lee, J. S. Chao, Material Science and Engineering B60 (1999), pp. 149-155.

[6] M. Ishimoto, R. Baragiola, and T. Shinoda, IDW’00 DIGEST, pp. 683-686 (2000).

[7] H.Uchiike, N.Nakayama, M.Ohsawa, ”Secondary Electron Emission Characteristics of Dielectric Materials in Plasma Display Panel”, IEEE Int. Electron Devices Meeting (IEDM), Digest, pp.191-194 (1973).

[8] D. Alpert and D. L. Bitzer, “Advances in computer-based education,” Science, Vol. 167, pp. 1582–1590 (1970).

[9] D. L. Bitzer, “Inventing the ac plasma panel,” Inf. Display, Vol. 15, pp. 22–27, (1999).

[10] D. L. Bitzer, H. G. Slottow, and R. H. Wilson, “Gaseous display and memory apparatus,” U.S. Patent 3 559 190, Jan. 26, 1971.

[11] R. H. Wilson, “A capacitively coupled bistable gas discharge cell for computer controlled display”, Univ. Illinois, Urbana-Champaign, Coordinated Sci. Lab. Rep. R-303, Jun. 1966.

[12] D. L. Bitzer and H. G. Slottow, “The plasma display panel-a digitally addressable display with inherent memory,” in Proc. Fall Joint Comput. Conf., Vol. 29, AFIPS Conf. Proc.,Washington, DC., pp. 541–547 (1966).

[13] E. Stredde, “The development of a multicolor plasma display panel”, University of Illinois, Coordinated Sci. Lab. Rep. R-370, Nov. 1967.

[14] J. F. Nolan, “Gas discharge display panel,” in Conf. Dig. Int. Elect. Dev. Meeting, Washington D.C., p. 54 (1969).

[15] R. L. Johnson, D. L. Bitzer, and H. G. Slottow, “The device characteristics of the plasma display element,” IEEE Trans. Electron Devices, Vol. ED-18, no. 9, pp. 642–649 (1971).

[16] G. E. Holz, “The primed gas discharge cell–A cost and capability improvement for gas discharge matrix displays,” in Proc. SID, vol. 13, pp. 2–5 (1972).

[17] G. Holz, “Pulsed gas discharged display with memory,” in Proc. SID Int. Symp., San Francisco, pp. 36–37 (1972).

[18] K. Kurahashi, H. Tottori, F. Isogai, N. Tsuruta, “Plasma display with grayscale,” in Proc. SID Int. Symp., New York, pp. 72–73 (1973).

[19] T. Kojima, R. Toyonaga, T. Sakai, T. Tajima, S. Sega, T. Juriyama, J. Koike, and H. Murakami, “Sixteen-in gas-discharge display panel with 2-lines-at-a-time driving”, in Proc. SID, Vol. 20, pp. 153–158 (1979).

[20] W. Miller, “Theory of penning ionization. I. atoms”, The Journal of Chemical Physics, Vol. 52, No.7, pp. 3563–3573 (1970).

[21] K. Yoshikawa, Y. Kanazawa, M. Wakitani, T. Shinoda, and O. Ohtsuka, “A full color ac plasma display with 256 grayscale,” in Japan Display Int. Display Res. Conf., Hiroshima, Japan, pp. 605–608 (1992).

[22] J. Johnson, K. McKay, “Secondary electron emission of crystalline MgO”, Physical Review, Vol. 91, No.3, pp. 582–587 (1953).

[23] H. Uchiike, N. Nakayama, and M. Ohsawa, “Secondary electron emission characteristics of materials in plasma display panels,” in Proc. Int. Electron Devices Meeting, Washington D.C., pp. 191–194 (1973).

[24] R. E. Ernsthausen and B.W. Byrum, “Gas discharge display and memory panel with magnesium oxide coatings,” U.S. Patent 3 863 089, Jan. 28, 1975.

[26] P. Pleshko, G. W. Smith, D. R. Thompson, and N. Vecchiarelli, “The characteristics and performance of an experimental ac plasma 960 ×768 line panel and electronics assembly,” in Proc. Int. Electron Devices Meeting, pp. 299 (1981).

[27] D. K. Wedding, P. S. Friedman, T. J. Soper, H. D. Holloway, and C. D. Reuter, “A 1.5-m-diagonal ac gas discharge display,” in Proc. SID Int. Symp., New Orleans, LA, pp. 96–99 (1987).

[28] T. Shinoda and A. Niinuma, “Logically addressable surface discharge ac plasma display panels with a new write electrode,” in Proc. SID Int. Symp., San Francisco, CA, pp. 172–175 (1984).

[29] L. F.Weber and M. B.Wood, “Energy recovery sustain circuit for the ac plasma display,” in Proc. SID Int. Symp., New Orleans, LA, pp. 92–95 (1987).

[30] T. Shinoda, “Fabrication technologies of plasma display panels”, Industry Applications Conference, 38th IAS Annual Meeting. Conference Record of the Publication Date: 12-16 Oct. 2003, Vol. 1, pp. 56- 61 (2003).

[31] T.Urade, T.Iemori, N.Nakayama, and I.Morita,:” Consideration of protection layer in AC plasma display panels”, Conf. Rec. IEEE-SID, 1974 Conf. Display Device and Systems,Oct.,pp.30-33 (1974).

[32] S.Hidaka, M.Ishimoto, N. Iwase, K.Betsui, and H.Inoue,;" Influence of Crystal Plane on the Sputtering Rate of MgO ", IDW'98, pp.523-526 (1998).

[34] M.Hakomori, Y. Hibino, K. Matsuzaki, M. Matsuura, and H.Yamakawa,;" High Rate Deposition of MgO Film for AC-PDP by Activated Reactive Evaporation Using Hollow Cathode Discharge (HCD-ARE)", IDW'97, pp.551-554 (1997).

[34] C.Daube, H. Frankenberger, J. Stollenwerk," High Rate MgO Sputter Source for PDP Application", IDW'97, pp.555-558 (1997).

[35] M. Ohring, "The Materials Science of Thin Films", Academic Press, New York (1992).

[36] Heung-Sik Tae, Jin-Won Han, Sang-Hun Jang, Byeong-No Kim, Bhum Jae Shin, Byung-Gwon Cho, and Sung-Il Chien, "Experimental Observation of Image Sticking Phenomenon in AC Plasma Display Panel", IEEE Trans. on Plasma Science, Vol. 32, No. 6, pp. 2189–2196 (2004).

[37] S.-H. Jang, K.-D. Cho, H.-S. Tae, K. C. Choi, and S.-H. Lee, "Improvement of luminance and luminous efficiency using address voltage pulse during sustain-period of AC-PDP," IEEE Trans. Electron Devices, vol. 48, pp. 1903–1910 (2001).

[38] T. Yamaguchi, T. Masuda, A. Kohgami, and S. Mikoshiba, "Degradation of moving-image quality in PDPs: Dynamic false contours," J. Soc. Inform. Display, vol. 4, no. 4, pp. 263–270 (1996).